Molecular characterization of superoxide dismutase and catalase genes, and the induction of antioxidant genes under the zinc oxide nanoparticle-induced oxidative stress in air-breathing magur catfish (*Clarias magur*)

Debaprasad Koner, Bodhisattwa Banerjee, Annu Kumari, Aquisha S.

Lanong, Revelbornstar Snaitang and Nirmalendu Saha*

Biochemical Adaptation Laboratory, Department of Zoology, North-Eastern Hill University, Shillong 793022, INDIA

*Corresponding author:

Prof. Nirmalendu Saha

Biochemical Adaptation Lab.

Department of Zoology

North-Eastern Hill University

Shillong 793022, INDIA

E-mail: nsaha@nehu.ac.in; nsahanehu@hotmail.com

Tel: +91 364 2722322

Orcid: 0000-0002-9635-3024

Abstract

The deduced amino acid sequences from the complete cDNA coding sequences of three antioxidant enzyme genes (cms*od1*, cms*od2*, and cm*cat*) demonstrated that phylogenetically the magur catfish (*Clarias magur*) is very much close to other bony fishes with complete conservation of active site residues among piscine, amphibian and mammalian species. The three-dimensional structures of three antioxidant enzyme proteins are very much similar to mammalian counterparts, thereby suggesting the functional similarities of these enzymes. Exposure to ZnO NPs resulted in an oxidative stress as evidenced by an initial sharp rise of intracellular concentrations of hydrogen peroxide (H_2O_2) and malondialdehyde (MDA), but decreased gradually at later stages. The level of glutathione (GSH) also increased gradually in all the tissues examined after an initial decrease. Biochemical and gene expression analyses indicated that the magur catfish has the ability to defend the ZnO NP-induced oxidative stress by inducing the SOD/CAT enzyme system and also the GSH-related enzymes that are mediated through the activation of various antioxidant-related genes both at the transcriptional and translational levels in various tissues. Furthermore, it appeared that the stimulation of NO, as a consequence of induction *nos2* gene, under NP-induced oxidative stress serves as a modulator to induce the SOD/CAT system in various tissues of magur catfish as an antioxidant strategy. Thus, it can be contemplated that the magur catfish possesses a very efficient antioxidant defensive mechanisms to defend against the oxidative stress during exposure to ZnO NPs into their natural environment, and also from related cellular damages.

Keywords: Antioxidant enzymes; Molecular phylogenetics; Inducible nitric oxide synthase; Hydrogen peroxide; Malondialdehyde, Glutathione

Introduction

Parallel to the increase of application of nanotechnology in recent years, more utilization of metal oxide nanoparticles (NPs) have received significant attention mainly because of their remarkable and multidimensional potentials. These metal oxide NPs are one of the most widely used nanomaterials in industrial and domestic applications (Aitken et al. 2006). But, at the same time, a large scale beneficial use of different metal oxide NPs has resulted in an uncontrolled release of these particles into the environment (Ray et al. 2009; Lin et al. 2010; Smita et al. 2012), thus causing an alarming increase of NPs into the surrounding environment as abiotic stress factors. Following the environmental release, the NPs are likely to enter into the aquatic ecosystem, which ultimately are causing a considerable load of different NPs in water bodies (Wigginton et al. 2007). Various pieces of evidence suggested that the NPs are potent aquatic pollutants since aquatic ecosystems

are the final destination for almost all anthropogenic discharges that flow through rainwater, which ultimately may have their adverse physiological effects on aquatic biota, including the fish species (Scown et al. 2010; Shaw and Handy 2011; Handy et al. 2011; Cazenave et al. 2019).

ZnO NPs are noncombustible, white, and odorless metal oxide powders. In recent years, ZnO NPs are known to be utilized extensively in industries and personal products due to their unique physicochemical characteristics (Zhang et al. 2013). ZnO NPs have been recognized as "extremely toxic" to aquatic organisms (Kahru and Dubourguier 2010); however, the toxicity level varies considerably to aquatic organisms belonging to various trophic levels (Blinova et al. 2010; Wong et al. 2010; Hanna et al. 2013). Several earlier studies demonstrated the embryotoxicity and developmental abnormalities under ZnO NPs exposure in zebrafish (*Danio rerio*), marine medaka (*Oryzias melastigma*), and daphnia (*Daphnia magna*) (Choi et al. 2016; Cong et al. 2017; Shin et al. 2018). Although many studies have elucidated the potential hazards of ZnO NPs to aquatic life and their environmental impacts, not much of information is available about the ZnO NP-induced cellular toxicity resulted due to overproduction of reactive oxygen species (ROS) and the possible endowed protective strategies. Some recent studies on common carp (*Cyprinus carpio*) and Nile tilapia (*Oreochromis niloticus*) have revealed the effects of ZnO NPs on bioaccumulation, oxidative stress, and the subsequent activation of the antioxidant defense system (Hao and Chen 2012; Kaya et al. 2015). In aquatic ecosystems, NPs are taken up by fish and transported to the various tissues and organs through the blood (Handy et al. 2008). In both *in vitro* and *in vivo* studies, it was demonstrated that ZnO NPs could induce oxidative stress by triggering ROS formation (Shahzad et al. 2019; Yang et al. 2020). Induction of oxidative stress causes extensive damage to biomolecules like DNA, proteins, lipids, and cellular membranes (Halliwell 1999). Oxidative stress in the cellular system is generated as a consequence of an imbalance between oxidative and reductive processes, and is typically induced when the physiological antioxidant defense system can no longer counteract the elevated ROS level (Zhao et al. 2009; Prieto et al. 2009), or as a result of the cellular incompetency to repair oxidative damages (Dorval 2003). Like other vertebrates, teleosts might have also evolved a wide array of enzymatic and non-enzymatic antioxidant defense systems to convert ROS to harmless metabolites to protect and restore normal cellular homeostasis and functions (Lushchak et al. 2001; Sinha et al. 2015). These include the low molecular weight antioxidants, such as glutathione (GSH), and high molecular weight defenses that have enzymes like superoxide dismutase (SOD), catalase (CAT) as the first line of defense, glutathione metabolism-related enzymes such as glutathione peroxidase (GPx), glutathione reductase (GR) and glutathione-S-transferase (GST), and glutathione reductase (GR) (Valavanidis et al. 2006; Lushchak 2011). Furthermore, the involvement of nitric oxide (NO), generally produced by nitric oxide synthase (NOS), to provide some

protection to the cellular system against the oxidative stress has been reported in goldfish (Hansen and Jensen 2010). However, the role of NO in defending against the NP-induced oxidative stress in different cellular systems of teleost fish is yet to be established except the recent report in primary hepatocytes of magur catfish under *in vitro* condition (Koner et al. 2019).

The facultative air-breathing magur catfish (*Clarias magur*, previously known as *Clarias batrachus*) is found predominantly in tropical Southeast Asia. They usually live in stagnant and slow-flowing sewage-fed polluted water bodies. They are likely to get exposed to NPs, including the ZnO NPs, in their natural habitats, mainly due to an infestation of industrial wastes and wide-scale anthropogenic activities. The magur catfish is more resistant to various environmental challenges such as high environmental ammonia, hypoxic, and desiccation stresses compared to any other typical teleosts (for reviews, see Saha and Ratha, 1998; 2007). Regardless of previous studies, the defensive strategies against the ZnO NP-induced oxidative stress in air-breathing catfishes and other teleosts have not been well studied. Thus, the primary purpose of the present study was (i) to determine the molecular characterization of SOD and CAT genes that are known to be involved as the first line of defense against oxidative stress, (ii) to investigate the level of oxidative stress caused due to exposure to ZnO NPs by quantifying the indices of oxidative stress such as hydrogen peroxide (H_2O_2), malondialdehyde (MDA), and reduced glutathione (GSH) in different cellular systems of magur catfish, and also (ii) to ascertain the antioxidant defense system in response to ZnO NPs exposure in different cellular systems/organs of magur catfish by analyzing the expression of certain antioxidant genes and their translated products along with the possible involvement of NOS/NO system in such defensive system against the ZnO NP-induced oxidative stress.

Materials and methods

Antibodies and reagents

A polyclonal antibody specific to inducible nitric oxide synthase (iNOS) was produced against the peptide from the epitope EIGARDFCDPQRYNILEKVGR. The peptide was conjugated to the KLH (Keyhole Limpet Hemocyanin) peptide to immunize the rabbit for obtaining the polyclonal antibody (Imagenex, India). The CAT (goat polyclonal) (cat # sc-34285), GPx (goat polyclonal) (cat # sc-22146), GST (rabbit polyclonal) (cat # sc-33613), TrxR (rabbit polyclonal) (cat # sc-20147), GAPDH (goat polyclonal) (cat # sc-48166), HRP-conjugated anti-goat (cat # sc- 2020) and anti-rabbit (cat # sc-2357) IgG were purchased from Santa Cruz Biotechnology, USA. Rabbit polyclonal SOD (cat # S4946) was procured from Merck, USA. Oligonucleotide primers were procured from GCC Biotech, India. Enzymes, coenzymes, substrates were procured from Sigma

Chemicals (St. Louis, USA). SYBR® Premix Ex Taq™ II was procured from Takara, Japan. Other chemicals were of analytical grades and obtained from local sources. MilliQ water was used in all preparations.

Experimental animal

The magur catfish (*C. magur*, weighing 140 – 160 g body mass) belonging to an age group of 18 – 24 months were purchased from a single source that was bred, cultured in selected commercial ponds of Nilbagan Fish Seed Farm situated in Barpeta, Assam, India. Fishes were acclimatized in the laboratory for approximately one month at 27 ± 2°C with 12 h:12 h light and dark photoperiod before experiments. No sex differentiation was done while performing these studies. Minced dry fish and rice bran (5% of body wt) were given as food every day, and the water, collected from a natural stream, was changed on alternate days. The study was approved by the Institutional Animal Ethics Committee (IAEC) of North-Eastern Hill University, Shillong, India (NEC/IEC/2018/016).

Total RNA extraction, cDNA synthesis

The total RNA was isolated from 50 mg of each tissue using TRI® Reagent (Sigma-Aldrich, St. Louis, USA), following the method of Rio et al. (2010), and quantified spectrophotometrically at 260 nm with the help of QIAxpert (Qiagen, Germany). The first-strand cDNA was synthesized from 400 ng of total RNA in a total volume of 20 µl with an iScript cDNA synthesis kit (Bio-Rad, USA) as per the standard protocol.

Sequencing and structural analysis of three antioxidant genes

Degenerate primers for three antioxidant enzyme genes (*sod1*, *sod2*, and *cat*) were designed from the conserved region of published sequences of different fish species. Partial sequencing of each gene was performed in 3130 Genetic Analyzer (Applied Biosystems, USA) using BigDye® Terminator v3.1 Cycle Sequencing Kit (Applied Biosystems, USA), followed by full-length sequences of *sod1*, *sod2*, and *cat* genes following 5′- and 3′-RACE-PCR with several gene-specific primers using the SMARTer RACE 5′/3′ Kit (Takara Clontech, Japan). All the primers used are described in Supplementary table T1. The open reading frame (ORF) was determined using the NCBI ORF finder (https://www.ncbi.nlm.nih.gov/orffinder/). The sequences were submitted to the GenBank with the following accession number: cm*sod1* (KF444052), cm*sod2* (MH891501), and cm*cat* (MW752164).

UTR motifs from the untranslated regions (UTRs) of the cDNAs were predicted by the UTRscan tool (Pesole et al. 2000). A Conserved Domain Database search (CD-search) was used for the identification of functional domains of the three antioxidant enzyme genes (cm*sod1*, cm*sod2*, and cm*cat*) (Marchler-Bauer et al.

2011). We used ProtParam (Gasteiger et al. 2005), ScanProsite (de Castro et al. 2006), and Motif Scan (Sigrist et al. 2010) tools on the ExPASy Server for determining the physicochemical properties and motifs of the translated amino acid (aa) sequences. The subcellular localization of the three genes was predicted by the MitoFates webserver (Fukasawa et al. 2015). Homology modeling of the three antioxidant enzymes was performed by SWISS-MODEL workspace (Schwede et al. 2003), and for quality assessment of the protein model QMEAN4 (Benkert et al. 2011) and PROCHECK (Laskowski et al. 1993) tools were used.

Multiple sequence alignments and phylogenetic analyses

Multiple sequence alignments of the inferred amino acids of the three enzymes from piscine, amphibian, and mammalian sequences using the M-coffee tool were performed (Moretti et al. 2007), followed by using of Gblocks program (Talavera et al. 2007) to eliminate poorly aligned positions and divergent regions of the alignments. Unrooted phylogenetic trees were constructed using the maximum-likelihood principle-based phylogeny with Smart Model Selection (PhyML + SMS) (Lefort et al. 2017) in the NGPhylogeny.fr web server (Lemoine et al. 2019).

Experimental setup

Initially, the magur catfish were exposed to different concentrations of ZnO NPs to determine the 96 h LC_{50} value, which was found to be 50 mg/L. Hence, it was decided to perform all the subsequent experiments with five times lesser concentration (10 mg/L) than the LC_{50} value, where no mortality was noticed even after 30 days of exposure.

Three sets of fish with 5 fish in each group were kept in four different plastic tumblers and administered to the aqueous suspension of ZnO NPs at a 10 mg/L concentration. Another set of 5 fish was held in a plastic tumbler containing 4 L of bacteria-free filtered stream water, which served as a control. The ZnO NP suspension was prepared in bacteria-free filtered stream water, where the NPs were dispersed by sonication for 6 h in a bath-type sonicator (100 W, 40 kHz). The ZnO NPs suspension and the bacteria-free filtered stream water were changed on alternate days at a fixed time. After 3, 7, and 14 days, 5 fish from treated and 5 control fish after 3 days were removed and killed by decapitation after anesthetizing in neutralized MS-222 (0.2 g/L) for 5 min. The liver, kidney, brain, muscle, and gills were dissected out and plunged into liquid nitrogen before storing at −80 °C. All analyses were completed within 3 weeks of collecting tissues. The experimental room temperature was maintained at 26 ± 2 °C with 12 h:12 h day and night photoperiods.

Quantification of H_2O_2, MDA, GSH, and NO concentrations

For quantification of H_2O_2, MDA, GSH, and NO concentrations in different tissues of both the control and treated fish, a 10% homogenate of each tissue were prepared in 50 mM Tris-HCl buffer (pH 7.4) containing a cocktail of protease inhibitor (Roche, Germany) using a motor-driven Potter-Elvehjem glass homogenizer with a Teflon pestle, followed by centrifugation at 10,000 × g for 10 min at 4 °C. The supernatant was used for various measurements. The H_2O_2 and MDA concentrations in the supernatant were measured by using Amplex® Red Hydrogen Peroxide/Peroxidase Assay Kit (Thermo Fisher, USA) and TBARS assay kit (DTBA-100, BioAssay Systems, USA), respectively, following manufacturers' instructions. The reduced glutathione (GSH) was measured in the supernatant, according to Ellman (1959). The yellow-colored mercapto-2-nitrobenzoic acid (TNB), formed as a product of the reaction between DTNB and GSH, was measured at 412 nm with a UV-visible spectrophotometer (Cary 60, Agilent, USA). To determine the concentration of NO, the supernatant was further treated with 5% perchloric acid (PCA) in a 1:0.5 ratio to precipitate out the proteins, followed by centrifugation again at 10,000× g for 5 min. The concentration of NO in the supernatant was determined by the Griess reaction described by Sessa et al. (1994). The purple azo product was measured spectrophotometrically at 540 nm with a UV-visible spectrophotometer (Cary 60, Agilent) against the reagent blank. The TBARS and NO concentrations were calculated using MDA and sodium nitrite, respectively, as reference standards.

The protein concentration in different tissues was determined using the Bradford reagent (Bradford 1976).

Enzyme assay

A 10% homogenate of each tissue was prepared in a homogenizing buffer containing 50 mM Tris-HCl (pH 7.5), 300 mM mannitol, 1 mM dithiothreitol (DTT), 1 mM ethylenediamine tetra-acetic acid (EDTA), and a cocktail of protease inhibitor (Roche, Germany). The homogenate was treated with 0.5 % Triton-X 100 in a 1:1 ratio for 30 min, followed by a mild sonication for 30 sec × 2. The homogenates were then centrifuged at 10,000 × g for 10 min, and the supernatant was used for assaying different enzyme activities. All the above steps were carried out at 4 °C.

The superoxide dismutase (SOD) and catalase (CAT) activities were assayed spectrophotometrically following Paoletti et al. (1986) and Beers and Sizer (1952), respectively. One unit of enzyme activity was defined as the amount of enzyme required to cause 50% inhibition of NBT photoreduction for SOD, and the amount of enzyme required to catalyze 1 μmole of H_2O_2 for CAT per min at 26 °C.

The glutathione-S-transferase (GST), glutathione peroxidase (GPx), and thioredoxin reductase (TrxR) activities were assayed spectrophotometrically following Habig et al. (1974), Chiu et al. (1976), and Holmgren

and Bjornstedt (1995), respectively. One unit of enzyme activity was defined as the amount of enzyme required to form 1 µmol of GSH-CDNB conjugate for GST, the amount of enzyme required to transform 1 µmol of NADPH to $NADP^+$ for GPx, and the amount of enzyme required to form 1 µmol of TNB for TrxR per min at 26 °C.

The inducible nitric oxide synthase (iNOS) activity was assayed spectrophotometrically following the method of Knowles and Salter (1998) with certain modifications made by Choudhury and Saha (2012). Citrulline, so formed as the reaction product, was estimated spectrophotometrically at 490 nm in a UV-visible spectrophotometer (Cary 60, Agilent, USA) following the method of Moore and Kauffman (1970) and expressed as enzyme activity. One unit of iNOS enzyme activity was defined as that amount of enzyme required to catalyse the formation of 1 µmole of citrulline per h at 26 °C

Quantitative real-time PCR (RT-qPCR) analysis

The real-time quantitative polymerase chain reaction (RT-qPCR) analysis was performed in a StepOne plus Real-time PCR system (Applied Biosystems, USA) using Premix Ex Taq II SYBR Green (Takara, Japan). The reaction mixture of 10 µl each contained 5 µl of SYBR Green Mix, 0.5 µl of cDNA, 400 nM of each primer, and MilliQ H_2O. The assay conditions included an initial denaturation step at 95 °C for 30 sec, followed by 40 cycles at 95 °C for 5 s and 60 °C for 34 s. The RT-qPCR was performed in triplicate for each sample, and negative controls using no cDNA were run for each gene. Melting curve analysis was used to confirm the amplification of only a single PCR product. The RT-qPCR products were sequenced in ABI 3130 Genetic Analyzer (Applied Biosystems, USA) to re-confirm the amplified product. Two reference genes (β-actin and α-tubulin) were selected, according to Banerjee et al. (2017). Fold changes of each gene were calculated using the modified ΔΔCT method (Livak and Schmittgen 2001). The used primer pairs were designed, and the specificity of each primer pair was checked using the Primer-BLAST tool (Ye et al. 2012) (Supplementary table T2).

Western blot analysis

Different tissues were homogenized in a lysis buffer (50 mM Tris-HCl pH 7.5, 300 mM sucrose, 1 mM EDTA, 0.1% SDS, 1% Triton X, 1 mM PMSF, protease inhibitor cocktail) and sonicated for 30 × 4 s. Lysates were centrifuged at 10,000×g for 10 min at 4 °C. For each tissue, 50 µg of cellular protein was resolved in 7.5% SDS-PAGE, followed by transferring the protein bands to the polyvinylidene fluoride (PVDF) membrane. Blots were probed using a specific antibody against the SOD, CAT, GPx, GST, TrxR, and iNOS enzyme proteins (1:5000 dilution), followed by incubation with HRP-conjugated secondary antibodies, and the

chemiluminescence was detected using Clarity™ Western ECL substrate (Bio-Rad, USA) in Image Quant LAS 500 system (GE Healthcare Life Sciences, USA). Glyceraldehyde 3-phosphate dehydrogenase (GAPDH) was used as a protein loading control.

Statistical analysis

The data, collected from different experiments, were statistically analyzed by a one-way ANOVA test to evaluate the significant differences obtained with relation to respective controls using GraphPad Prism software and presented as mean ± SEM (n = 5 in each set of the experiment). Differences with $P<0.05$ were regarded as statistically significant. Levene's test was also performed to verify the homogeneity of variance of different parameters between the control and treated groups of each experiment set.

Results

Identification and characterization of three antioxidant enzyme genes

Partial sequencing, followed by full-length 5′ and 3′ RACE-PCR of *cmsod1*, *cmsod2,* and cm*cat* produced complete cDNA sequences of these three antioxidant enzyme genes. The sequence of cms*od1* consisted of 741 nt encoding a 154 aa protein, cms*od2* consisted of 1033 nt encoding a 224 aa protein. Similarly, the cm*cat* sequence consisted of 3023 nt encoding 526 aa protein. The UTRscan tool predicted the presence of an Internal Ribosome Entry Site (IRES) in all three genes. Table 1 consisted of the detailed characteristics of full-length cDNAs for the antioxidant enzyme genes.

ScanProsite tool predicted the presence of two motif (Copper/Zinc superoxide dismutase signature) with a consensus pattern of [GA]-[IMFAT]-H-[LIVF]-H-{S}-x-[GP]-[SDG]-x-[STAGDE] and G-[GNHD]-[SGA]-[GR]-x-R-x-[SGAWRV]-C-x, respectively, in the cms*od1* aa sequence. The conserved domain search predicted a single conserved domain (Cu-Zn_Superoxide_Dismutase) with several Cu^{2+} and Zn^{2+} binding sites. In the case of the cms*od2* aa sequence, a single motif (Manganese and iron superoxide dismutases signature) was predicted with a consensus pattern of D-x-[WF]-E-H-[STA]-[FY]. Similarly, the conserved domain search also predicted a single conserved domain (SodA; Superoxide dismutase).

Multiple sequence alignment of derived aa sequences of cms*od1*and cms*od2* with some piscine, amphibian, bird, and mammalian sequences exhibited conservation of all the motif residues (Fig. 1, 2). The multiple protein alignment of SOD1 (Cu/Zn-SOD) protein (derived aa sequences of cms*od1*) showed the highest sequence identity (87%) with another air-breathing stinging catfish (*Heteropneustes fossilis*), followed by two catfishes such as striped catfish (*Pangasianodon hypophthalmus*) and channel catfish (*Ictalurus punctatus*) with 86% and

82% identities, respectively, and 83% sequence identity with the Mexican tetra (*Astyanax mexicanus*). MitoFates predicted the presence of a mitochondrial processing peptidase (MPP) cleavage site (26th residue of aa sequence), TOM20 recognition motif (8- 12 aa residues), and amphipathic alpha-helix in the aa sequence of SOD2 (Mn-SOD) protein, thus predicting mitochondrial localization of the protein. The multiple protein alignment of SOD2 protein (derived aa sequences of cm*sod2*) exhibited the highest sequence identity of 94% with another air-breathing stinging catfish (*H. fossilis*), followed by two other catfish such as striped catfish (*P. hypophthalmus*) and channel catfish (*I. punctatus*) with 92% identity.

The sequence of cm*cat* consisted of 3187 nt encoding a 526 aa protein. The motif search with the ScanProsite tool predicted the presence of two motifs; catalase proximal active site signature with a consensus pattern [IF]-x-[RH]-x(4)-[EQ]-R-x(2)-H-x(2)-[GAS]-[GASTFY]-[GAST], and catalase proximal heme-ligand signature with a consensus pattern R-[LIVMFSTAN]-F-[GASTNP]-Y-x-D-[AST]-[QEH] in the cm*cat* aa sequence. The conserved domain search also predicted one conserved domain (catalase_clade_3) with several heme-binding sites. Multiple sequence alignment of derived aa sequences of cm*cat* with some piscine, amphibian, bird, and mammalian sequences exhibited conservation of all the motif residues (Fig. 3). The amino acid sequence alignment exhibited a high sequence identity (96 - 92%) with the stinging catfish (*H. fossilis*), striped catfish (*P. hypophthalmusi*), and channel catfish (*I. punctatus*), 90% sequence identity with the Mexican tetra (*A. mexicanus*), zebrafish (*D. rerio*), fugu (*Takifugu* rubripes), 80% identity with the elephant shark (*Callorhinchus milii*), and 78% identity with the mammalian sequences.

Structural analysis

The ProtParam tool predicted a theoretical pI of 5.94, 8.35, and 8.34 and the MW of 15.9, 25.08, and 59.8 kDa of the derived aa sequences of *sod1*, *sod2,* and *cat* genes, respectively. The homology modeling of SOD1 is predicted as homo-dimer protein. At the same time, SOD2 and CAT were predicted both as homo-tetrameric proteins. The predicted model for SOD1 was based on human-mouse SOD1 chimera (3gtv.1) with 72.37% of sequence homology (Fig. 4a). The predicted model for SOD2 was based on human mitochondrial MN3+ superoxide dismutase (1n0j.1) with 84.3% of sequence homology (Fig. 4a). Similarly, beef liver catalase (7cat.1) with 81.3% sequence homology was used as the CAT model template (Fig. 4a). Structural analysis revealed the putative metal-binding sites of the SOD1 (four residues for Zn^{2+} binding: H64, H72, D84, and H81) and SOD2 (four residues for Mn^{2+} binding: H52, H100, D185, and H189) (Fig. 4b). The Ramachandran plot of phi-psi torsion angles showed that 99.34%, 96.68%, and 94.76% of residues were in the most favored regions of SOD1, SOD2, and CAT models, respectively (Fig. 4c).

Phylogenetic analysis

The molecular phylogenetic analysis of the three antioxidant enzymes was performed using the PhyML algorithm. Phylogenetic analysis of several vertebrate SOD1 and SOD2 enzymes displayed two large clusters, one with the teleost group and another cluster represented the mammalian, amphibian, bird, and elasmobranch (Fig. 5). Furthermore, the phylogenetic analysis of CAT from different vertebrates showed a similar pattern, where all the teleost CAT were clustered together, and another cluster represented the mammalian, bird, and elasmobranch sequences (Fig. 5).

Changes in cellular concentrations of H_2O_2, MDA, and GSH

Exposure to ZnO NPs led to a sharp rise in the intracellular concentration of H_2O_2 in different tissues of magur catfish within 3 days, followed by a gradual decrease at later stages, reaching almost to the basal level after 14 days of exposure (Fig. 6a). It increased maximally by 2.3-fold in the liver, 2.2-fold in the kidney, 2.0-fold in the brain and muscle, and 2.2-fold in the gills after 3 days of exposure than untreated controls. Similarly, a sharp rise of MDA level was also observed in different tissues of magur catfish within 3 days of exposure to ZnO NPs, later followed by a gradual decrease. Still, it remained significantly higher than the respective control values even after 14 days of exposure (Fig. 6b). It increased maximally in the liver, kidney, brain, muscle, and gills by 1.7-, 1.8-, 2.7-, 2.6-, 6.5-fold, respectively, after 3 days of exposure compared to untreated controls. Whereas the GSH level in different tissues of ZnO NP-treated magur catfish was found to decrease significantly until 7 days, but on 14 days, it was found to increase considerably in all the tissues (Fig. 6c). It increased significantly by 1.5-, 1.4-, 1.3-, 1.4- and 1.3-fold in the liver, kidney, brain, muscle, and gills, respectively, after 14 days of treatment.

Changes in activities of antioxidant enzymes

The changes of activities of different antioxidant enzymes in various tissues of magur catfish while exposing to ZnO NPs compared to untreated controls are presented in Fig. 7. The activities of both SOD and CAT enzymes were seen to decrease initially in different tissues within 3 days of treatment, followed by a gradual and significant rise of activities at later stages of treatment. In the case of SOD, the activity increased maximally by 1.3-, 1.5-, 1.4-, 1.9- and 1.6-fold in the liver, kidney, brain, muscle, and gills, respectively, after 14 days of treatment compared to untreated controls. In the case of CAT, the activity increased maximally in the liver and brain by 2-fold, followed by in the kidney (1.9-fold), muscle (1.8-fold), and gills (1.6-fold) after 14

days of treatment compared to untreated control values. Whereas, in the case of GSH metabolism-related enzymes such as the GST, GPx, and TrxR, the activities were found to increase significantly within 3 days of treatment, followed by a further rise of activities at later stages of treatment. Compared to untreated controls, the GST activity increased maximally by 1.8-fold in the liver, followed by in the kidney and muscle (1.6-fold), brain (1.5-fold), and in the gills (1.4-fold) after 14 days of exposure to ZnO NPs. In the case of GPx, the activity increased maximally in the liver, kidney, brain, muscle, and gills by 1.8-, 1.4-, 2.0- 1.7-, and 1.2-fold, respectively, after 14 days of exposure compared to untreated controls. Similarly, the activity of TrxR was also found to increase maximally by 3.1-, 3.0-, 2.5-, 1.8- and 1.7-fold in the liver, brain, kidney, muscle, and gills, respectively, after 14 days of treatment compared to untreated controls.

Changes in the expression of antioxidant enzyme genes

The relative abundance of mRNAs for different antioxidant genes was measured by RT-qPCR analysis to assess the possible changes in gene expression in various tissues of magur catfish during exposure to ZnO NPs, (Fig. 8). In general, the expression of mRNAs for different antioxidant enzyme genes increased significantly in most of the tissues of treated fish compared to untreated controls at variable levels. The maximum increase in mRNA expression for *sod1* gene was seen in the muscle and brain by 2.4- and 2.3-fold, respectively, after 3 days, followed by in the kidney (1.9-fold), liver (1.8-fold), and gills (1.6-fold) after 14 days of treatment. The level of *sod2* mRNA increased maximally by 3.2-fold in the liver, followed by in the kidney (2.9-fold), gills (2.8-fold), brain (2.6-fold), and muscle (2.5-fold) after 14 days of exposure. In the case of *the cat* gene, the mRNA expression increased maximally in the brain and gills by 2.5-fold, followed by in the kidney (2.4-fold), liver (2.3-fold), and muscle (2.1-fold) after 14 days of treatment compared to untreated controls. The expression of mRNA for the *gst* gene increased maximally in the kidney by 3.4-fold after 7 days, followed by the liver, muscle, brain, and gills by 2.6-, 2.3-, 2.2- and 1.9-fold. The *gpx1* mRNA level increased maximally in the muscle by 3.9-fold, followed by in the brain (3.6-fold), liver (2.3-fold), gills (2.2-fold), and kidney (2.1-fold) after 14 days of exposure. In the case of the *txnrd1* gene, the mRNA level increased significantly within 3 days, which later increased further to a maximum level by 3.1-fold in the liver, followed by in the brain (2.6-fold), muscle (2.5-fold), gills (2.1-fold), and kidney (1.9-fold) after 14 days of exposure.

Changes in the expression of antioxidant enzyme proteins

Western blot analysis demonstrated that the exposure of magur catfish to ZnO NPs also led to a significant rise in the expression of different antioxidant enzyme proteins in various tissues compared to

untreated controls (Fig. 9a, b). The SOD enzyme protein level increased maximally by 2.7-fold in the kidney, followed by the liver by 2.6-fold, brain, and gills by 2.3-fold, and in the muscle, it increased by 2.2-fold after 14 days of treatment. The increase of the relative abundance of CAT enzyme protein also occurred in all the tissues examined with a maximum rise by 2.2-fold in the liver, followed by in the kidney (2.1-fold), gills (2.0-fold), muscle (1.8-fold), brain (1.7-fold) after 14 days. The GST enzyme protein also displayed the highest increase in its expression in the kidney by 2.7-fold after 7 days, followed by the liver, muscle, gills, and brain by 2.4-, 2.1-, 1.9-, and 1.7-fold, respectively, after 14 days of exposure. The maximum increase in the expression of GPx enzyme protein was observed in the muscle, brain, gills, liver, and kidney by 3.2-, 3.1-, 2.2-, 2.5-, and 2.1-fold, respectively, after 14 days of exposure. Similarly, the expression of TrxR enzyme protein also increased significantly with a maximum rise in the liver, muscle, brain, kidney, and gills by 2.4-, 2.2-, 1.9-, 1.7- and 1.6-fold, respectively, after 14 days of exposure.

Changes in the concentration of NO and iNOS actvity

A relatively low level of NO was recorded in different tissues of control magur catfish, which increased significantly at variable levels in multiple fish tissues within 3 days of exposure to ZnO NPs, followed by a further rise at later stages of exposure (Fig. 10a). It increased maximally in the muscle by 5.0-fold, followed by in the gills, kidney, and liver by 4.5-, 2.2- and 2.1-fold, respectively, after 14 days, and in the brain, it increased maximally by 1.7-fold after 7 days of exposure.

The iNOS activity could not be detected in any of the control fish tissues examined. However, after treating with ZnO NPs, a significant level of iNOS activity could be seen in all the tissues examined within 3 days, which increased further at later stages of treatment (Fig. 10b). While comparing the relative level of activity of iNOS in different tissues, the maximum activity was seen in the kidney (18.3 units/g wet wt), followed by in the liver (12.2 units/g wet wt), brain (5.3 units/g wet wt), gills (4.2 units/g wet wt), and muscle (2.4 units/g wet wt) after 3 days of treatment with ZnO NPs. The iNOS activity enhanced further at later stages of treatment with a maximum rise by 3.3-, 2.6-, 3.4-, 4.0-, 3.7-fold, respectively, in the liver, kidney, brain, muscle, and gills after 14 days while comparing with the 3 days exposed fish.

Changes in the expression of *nos2* mRNA and iNOS protein

Fishes exposed to ZnO NPs, led to a significant increase in *nos2* mRNA expression in different tissues within 3 days, followed by a further rise at later stages (Fig. 10c). The *nos2* mRNA level increased maximally in

the kidney by 12.4-fold, followed by the muscle (4.6-fold) and brain (4.4-fold) after 7 days. Whereas, in the liver and gills, it increased maximally by 9.0- and 8.6-fold, respectively, after 14 days of exposure.

We could not detect any visible immunoreactive iNOS protein band in any of the tissues of untreated control fish examined by Western blotting. However, after exposing the fish to ZnO NPs, prominent immunoreactive bands of approximately 130 kDa could be detected in all the tissues with a further rise of band intensities at later stages of exposure (Fig. 10d). Densitometric analysis of protein bands revealed that the expression of iNOS protein increased maximally in the kidney by 3.7-fold, followed by in the liver, muscle, gills, and brain by 3.4-, 1.7-, 1.6-fold, respectively, after 14 days of exposure to ZnO NPs (Fig. 10e).

Discussion

In the present study, we report here the full nucleotide and the translated amino acid sequences of three antioxidant enzyme genes, such as the cm*sod1*, cm*sod2*, and cm*cat*, and also some of the molecular characteristics of these genes in magur catfish (*C. magur*). Unlike highly structured introns, the UTRs of mRNAs are not generally evolved to adopt single, well-defined structures; however, UTRs contain several gene regulatory elements (Barrett et al. 2012). These UTRs mainly control the translation and RNA decay and act as targets for RNA interference (Halvorsen et al. 2010). The presence of IRES motifs suggests an alternative ribosomal binding site for translation initiation (Le and Maizel 1997), and all the antioxidant enzyme genes (cm*sod1*, cm*sod2*, and cm*cat*) contained this motif. The Musashi protein is an evolutionarily conserved protein necessary for regulating the temporal order of mRNA translation (Charlesworth et al. 2006). The presence of MBE-box in *cmsod1*, *cmsod2*, and cm*cat*, suggests that the Musashi protein remains bound to these genes and regulate their translational processes.

The subcellular localization prediction confirmed the presence of a putative mitochondrial targeting sequence in the N-terminal region of SOD2 aa sequence, deduced from cm*sod2* gene. Therefore Cm-SOD2 was predicted to be mitochondrial SOD (Mn-SOD), similar to Mn-SODs reported from spotted barbell (*Hemibarbus mylodon*) (Cho et al. 2009), zebrafish (*Danio rerio*) (Lin et al. 2009), large yellow croaker (*Pseudosciaena crocea*) (Liu et al. 2015) and olive flounder (*Paralichthys olivaceus*) (Wang et al. 2011).

The crystal structure of human-mouse SOD1 chimera (3gtv.1), human mitochondrial MN3+ superoxide dismutase (1n0j.1), and beef liver catalase (7cat.1) with very high sequence homologies were identified as the best template for magur catfish SOD1, SOD2, and CAT, respectively, in homology modeling by the Swiss-Model workspace. The amino acids coordinated for the metal ion binding in SOD1 and SOD2 were found to be highly conserved across species (Lin et al. 2009; Umasuthan et al. 2014). The three antioxidant enzyme protein

models' Ramachandran plots showed that the Phi- and Psi-angles for most residues are in the most favored region, demonstrating a high-quality model. These findings strongly indicated that the three-dimensional structures of three antioxidant enzyme proteins are like their mammalian counterparts, suggesting the functional similarities of these enzymes in antioxidant defense.

The molecular phylogenetic analysis of the three antioxidant enzymes was also performed with known selected vertebrates. Phylogenetic analysis of SOD1 and SOD2 displayed two large clusters, where all the teleost SODs, including the *C. magur*, belonged to one cluster, and mammalian, amphibian, and elasmobranch were in another cluster. The phylogeny of CAT also showed a similar pattern. In all the phylogenetic trees, the nearest neighbor of the magur catfish is another catfish, *H. fossilis*. Two other catfish (*I. punctatus* and *P. hypophthalmus*) were also present as neighbors. Indeed, it is very much evident that a close relationship exists between these two antioxidant enzymes of air-breathing C. *magur* with other freshwater catfishes, and to some extent, with other teleosts rather than those of lungfishes and cartilaginous fishes.

Furthermore, the amino acid sequence homology between these three antioxidant enzymes of *C. magur* and other vertebrates showed a high degree of conservancy. Specifically, the functional domains and active site residues were all conserved across species. The conservation appeared to be justified since the active site residues are required for the enzyme functionality.

Moreover, the sequence alignments amino acid of these three vertebrate antioxidant enzyme proteins showed a high degree of sequence homology between the magur catfish and the other bony fishes (average of 92%). A complete amino acid conservation in functional domains across the species was also observed. Furthermore, the alignments demonstrated complete conservation of active site residues in all the three antioxidant enzyme proteins among piscine, amphibian, and mammalian species, which appeared to be justified since the active site residues are required for the functionality of the enzyme.

The results from the present study clearly demonstrated that exposure of magur catfish to a sub-lethal dose of ZnO NPs (10 mg/L) resulted in an initial rise of ROS production, causing oxidative stress, as evidenced by a sharp increase in the intracellular concentrations of both H_2O_2 and MDA at variable levels in different tissues examined. However, it is to be noted that the elevated levels of H_2O_2, which reached a peak on day 3, gradually decreased almost to the basal level at later stages of treatment. Further, excess of H_2O_2 (and $O_2^{\bullet-}$), which can be transformed to form highly reactive oxidant hydroxyl radicals ($^{\bullet}OH$) via the Harber-Weiss reaction, generally leads to lipid peroxidation through degradation of polyunsaturated fatty acids (PUFAs). Hence, we could also observe a significant rise in malondialdehyde (MDA) concentration, the oxidative end product of PUFAs, in different tissues of magur catfish examined in response to ZnO NPs exposure with a peak of increase within 3

days, followed by a gradual decrease at later stages of treatment. However, compared to H_2O_2, it maintained a higher level even after 14 days of treatment against the untreated control values. In general, the nano form of various metal ions produces more ROS than their bulk counterparts in cellular systems due to their unique physicochemical characteristics (Fu et al. 2014). Similar to our findings, elevated production of ROS and subsequent oxidative damages by ROS during exposure to nano-scale of TiO_2 and ZnO have also been reported in zebrafish (*D. rerio*) (Xiong et al. 2011). Several studies on mechanistic pathways illustrating the significant role of dissolved intracellular Zn^{2+} in ROS production and subsequent oxidative stress during exposure to ZnO NPs have also been reported (Kao et al. 2012; Buerki-Thurnherr et al. 2013). Similarly, ZnO particle size-dependent cellular damages have also been reported in tilapia (*Oreochromis niloticus*) and the increase in the levels MDA in different tissues due to increased production of ROS (Kaya et al. 2016). Thus, it is apparent that more accumulation of MDA in various tissues of magur catfish at variable levels, observed during *in situ* exposure to ZnO NPs, was associated with elevation of lipid peroxidation in response to NP-induced oxidative stress.

GSH is one of the most abundant intracellular antioxidant thiols, which is known to act as a substrate or cofactor for various enzymatic reactions of the glutathione-dependent cycle, decomposition of H_2O_2 to water, and in the reduction of lipid peroxidation. Further, it is known to get involved in cellular redox homeostasis by quenching superoxides and is central to defensive mechanisms against toxic agents and oxidant-mediated injury (DeLeve and Kaplowitz 1991; Townsend et al. 2003). Our present study observed that the GSH level decreased at the initial stages of treatment with ZnO NPs in all the tissues of magur catfish examined, which increased at later stages with a peak of increase after 14 days of exposure. The initial depletion of the GSH level was probably associated with the rise of ZnO NPs-induced ROS production in different tissues. A drastic drop in the level of GSH at the early stages of exposure indicated a condition of oxidative stress inside the cell as a consequence of imbalance in the ROS formation and antioxidant defense system within the cellular system (Guan et al. 2012). This observation is consistent with the reports that GSH is consumed in many ways, such as oxidation, conjugation, hydrolysis, and GSH can be directly oxidized by ROS and RNS, or indirectly during GSH-dependent peroxidase-catalyzed reactions (Kohen and Nyska 2002; Lushchak 2012). Similarly, Sarkar et al. (2017) also demonstrated the depletion of GSH levels in zebrafish liver and kidney under arsenic trioxide-induced oxidative stress. Similar to our findings, exposure to silver nanoparticles (Ag-NPs) was reported to cause an initial decrease in GSH level in brain tissue of two fishes (*Oreochromis niloticus* and *Tilapia zillii*), followed by a gradual increase of GSH level at later stages (Afifi et al. 2016). Thus, the initial depletion of GSH level in different tissues of magur catfish, observed during exposure to ZnO NPs, was probably associated with

to quench the superoxides, followed by a significant elevation of its level at later stages due to induction of GSH synthetic pathway, and also other antioxidant pathways (discussed later) in different tissues of magur catfish mainly to defend against the ZnO NP-induced oxidative stress.

Various antioxidant defense systems have been evolved in different organisms to fight against the free radical-mediated cellular damages and also to maintain redox homeostasis. Out of those, specific enzymatic systems are known to work as antioxidants in different cellular systems; this includes the SOD/CAT enzymes as the first line of defense, and also certain glutathione-dependent enzymes like the GST, GPx, and GR (Birben et al. 2012). In the present study, we observed an initial decrease of SOD and CAT activities in different tissues within 3 days of exposure to ZnO NPs, thus causing a higher accumulation of free radicals, leading to increased H_2O_2 and MDA concentrations in various tissues. But, the activities of both the enzymes increased significantly at later stages of exposure to ZnO NPs at variable levels in different tissues examined, which eventually were able to scavenge the elevated levels of ROS and ameliorate the ZnO NPs-induced oxidative damages to a certain extend. Other than the SOD and CAT, we also observed a gradual increase in the activities of glutathione-dependent antioxidant enzymes like GST and GPx in different tissues during exposure to ZnO NPs. Exposure to ZnO NPs also caused an increase in the activity of thioredoxin reductase (TrxR) in various tissues, which we speculated as an alternative to glutathione reductase (GR) for the maintenance of the GSH pool in this magur catfish. The transcriptome analysis of this magur catfish revealed the absence of any gene for the GR enzyme and the presence of the TrxR (*txnrd1*) gene (Banerjee et al. 2019). Further, we also could not detect the GR activity in any of the tissues of magur catfish examined. The annotated genome sequence of a closely related channel catfish (*I. punctatus*) (GCF_001660625.1) also revealed the absence of any gene for GR (Liu et al. 2016). Studies in *Drosophila melanogaster* and *Saccharomyces cerevisiae* demonstrated the role of TrxR as a substitution for GR (Kanzok 2001; Tan et al. 2010). Sakurai et al. (2005) also reported that TrxR is an essential component of the Trx system in the cytosol of bovine endothelial cells, which is induced under oxidative stress.

Interestingly, the increase of antioxidant enzyme activities was accompanied by a significant rise in the expression of all the antioxidant enzyme genes (*sod1*, *sod2*, *cat*, *gst*, *gpx1* and *txnrd1*) during exposure to ZnO NPs, as evidenced by more abundance of mRNA levels of all the genes at variable levels in different tissues of magur catfish. The *sod1* and *sod2* mRNA levels increased significantly in various tissues, but the level of induction of *sod2* (mitochondrial) was higher than the *sod1* (cytosolic) in all the tissue examined. Previous studies also demonstrated a higher level of induction of the *sod2* gene than other forms of *sod*, and are highly regulated by a variety of intracellular and environmental cues (Zelko et al. 2002). Similarly, the levels of

mRNAs for *cat*, *gst*, *gpx1,* and *trxnrd1* genes also increased significantly in different tissues of magur catfish during exposure to ZnO NPs. The whole transcriptome analysis, carried out under ammonia-induced oxidative stress in the liver and brain tissues of magur catfish, also demonstrated the possible induction of a set of antioxidant genes (Banerjee et al. 2019). The increase in concentrations of mRNAs for different antioxidant genes was also supplemented by a significant rise in the abundance of various antioxidant enzyme proteins at variable levels in all the tissues examined during exposure to ZnO NPs. Thus, it may be contemplated that both the transcriptional and translational activation of different antioxidant genes took place for the active scavenging of free radicals and to counteract the redox imbalance in this catfish under NP-induced oxidative stress. However, it is to be noted that the increase of mRNA levels of most of the antioxidant genes was relatively higher compared to the rise in enzyme protein levels and also the enzymatic activities under NP-induced oxidative stress. Thus, it appeared that there occur some translational and post-translational regulatory mechanisms to regulate these enzymes are probably functioning in this catfish to regulate the activities of these enzymes. Nonetheless, the present findings clearly demonstrated that the magur catfish has the ability to defend itself against the ZnO NPs-induced oxidative stress by inducing different antioxidant-related genes as a unique biochemical adaptational strategy.

More recently, the antioxidant activity of NO against the ammonia- and ZnO NP-induced oxidative stress has been demonstrated in primary hepatocytes of magur catfish (Koner et al. 2019; Hasan et al. 2020). Therefore, in the present study, we also looked at the possible induction of NO synthesis via the NO/NOS system in various tissues of magur catfish while exposing the fish to a sub-lethal dose of ZnO NP. Interestingly, exposure to ZnO NPs also led to a continuous increase of NO concentration at variable levels in different tissues, with having a maximum accumulation after 14 days of exposure in most of the tissues examined. This finding was further supplemented by the observations made on the stimulation of iNOS activity, up-regulation of the *nos2* gene, and more abundance of its translated enzyme protein at variable levels in different tissues of magur catfish. In our previous studies, we have fairly demonstrated that the induction of both SOD and CAT genes under ammonia- and NP-induced oxidative was mediated by the NO, the production of which was stimulated via the NFκB- mediated induction of NO/NOS system, as an antioxidant strategy (Koner et al. 2019; Hasan et al. 2020). The induction of NO synthesis via the NOS/NO system has also been reported in non-hepatic tissues of this magur catfish under hyper-ammonia stress, and also while treating with lipopolysaccharide (Choudhury et al. 2018; Kumari et al. 2019). Therefore, it is logical to think that NO is playing a vital role in defending against the NP-induced oxidative stress in different tissues of magur catfish, other than the hepatocytes, at least by stimulating the SOD/CAT system. However, one has to look into the involvement of NO in the induction of

glutathione pathway-related genes in this catfish under NP- and probably under other environmentally-induced oxidative stress.

Conclusion

We performed the full nucleotide and translated amino acid sequences of three different antioxidant enzyme genes (cm*sod1*, cm*sod2*, and cm*cat*) in air-breathing magur catfish (*C. magur*). The sequence alignment of amino acids of these three antioxidant enzyme proteins of magur catfish showed a high degree of sequence homology with that of other bony fishes along with complete conservation of active site residues in all the three enzyme proteins among piscine, amphibian and mammalian species. The three-dimensional structures of three antioxidant enzyme proteins are very much like their mammalian counterparts, thereby suggesting the functional similarities of these enzymes in antioxidant defense. The phylogenetic analysis of the three enzyme proteins indicated that *C. magur* is closely related to all bony fishes with more of similarities with other related catfishes. Furthermore, it is strongly suggested that the magur catfish has the ability to reduce the ZnO NP-induced oxidative stress by inducing the SOD/CAT enzymatic system, and also the GSH pathway-related enzymes as a consequence of induction of related genes both at the transcriptional and translational levels in various tissues. Furthermore, it appeared that the stimulation of endogenous NO production, which is mediated through the induction *nos2* gene under NP-induced oxidative stress, served as a modulator for the induction of SOD/CAT system in various tissues apart from the liver tissue of magur catfish as an antioxidant strategy. However, the role of NO in the induction of GSH pathway is yet to be established under NP-induced oxidative stress in this air-breathing catfish. Nonetheless, it is very much evident that the magur catfish possesses a very efficient antioxidant defensive mechanisms to defend against the NP-induced oxidative stress and also from related cellular damages.

Acknowledgment

The authors thank the Head, Department of Zoology, North-Eastern Hill University, Shillong for allowing us to use the instrumentation facilities in the Department in carrying out different experiments and analyses.

Data availability

Data are available from corresponding author upon reasonable request.

Author Contributions

D.K.: Methodology, investigation, formal analysis, writing the original draft; **B.B:** Methodology and investigation. **A.K.:** Methodology and investigation. **A.S.L:** Methodology and investigation**. R.S.:** Methodology

and investigation. **N.S.:** Conceptualization, validation, formal analysis, investigation, resources, data curation, writing - review & editing, supervision, project administration and funding acquisition.

Funding Sources

This work was supported by a research project sanctioned to NS by the Science and Engineering Research Board, New Delhi, India` (EMR/2016/005263).

Declarations

Ethics approval

The study was approved by the Institutional Animal Ethics Committee (IAEC) of North-Eastern Hill University, Shillong, India (NEC/IEC/2018/016).

Consent to participate

Not applicable.

Consent for publication

Not applicable.

Conflict of interest

The authors declare no competing interests.

References

Afifi M, Saddick S, Abu Zinada OA (2016) Toxicity of silver nanoparticles on the brain of *Oreochromis niloticus* and *Tilapia zillii*. Saudi J Biol Sci 23:754–760. https://doi.org/10.1016/j.sjbs.2016.06.008

Aitken RJ, Chaudhry MQ, Boxall ABA, Hull M (2006) Manufacture and use of nanomaterials: current status in the UK and global trends. Occup Med (Chic Ill) 56:300–306. https://doi.org/10.1093/occmed/kql051

Banerjee B, Koner D, Hasan R, et al (2019) Transcriptome analysis reveals novel insights in air-breathing magur catfish (*Clarias magur*) in response to high environmental ammonia. Gene 703:35–49. https://doi.org/10.1016/j.gene.2019.04.009

Banerjee B, Koner D, Lal P, Saha N (2017) Unique mitochondrial localization of arginase 1 and 2 in hepatocytes of air-breathing walking catfish, *Clarias batrachus* and their differential expression patterns under hyper-ammonia stress. Gene 622:13–22. https://doi.org/10.1016/j.gene.2017.04.025

Barrett LW, Fletcher S, Wilton SD (2012) Regulation of eukaryotic gene expression by the untranslated gene regions and other non-coding elements. Cell Mol Life Sci 69:3613–3634. https://doi.org/10.1007/s00018-012-0990-9

Beers RF, Sizer IW (1952) A spectrophotometric method for measuring the breakdown of hydrogen peroxide by catalase. J Biol Chem 195:133–40

Benkert P, Biasini M, Schwede T (2011) Toward the estimation of the absolute quality of individual protein structure models. Bioinforma 27:343–350. https://doi.org/10.1093/bioinformatics/btq662

Birben E, Sahiner UM, Sackesen C, et al (2012) Oxidative stress and antioxidant defense. World Allergy Organ J 5:9–19. https://doi.org/10.1097/WOX.0b013e3182439613

Blinova I, Ivask A, Heinlaan M, et al (2010) Ecotoxicity of nanoparticles of CuO and ZnO in natural water. Environ Pollut 158:41–47. https://doi.org/https://doi.org/10.1016/j.envpol.2009.08.017

Bradford MM (1976) A rapid and sensitive method for the quantitation of microgram quantities of protein utilizing the principle of protein-dye binding. Anal Biochem 72:248–254. https://doi.org/10.1016/0003-2697(76)90527-3

Buerki-Thurnherr T, Xiao L, Diener L, et al (2013) In vitro mechanistic study towards a better understanding of ZnO nanoparticle toxicity. Nanotoxicology 7:402–416. https://doi.org/10.3109/17435390.2012.666575

Cazenave J, Ale A, Bacchetta C, Rossi AS (2019) Nanoparticles toxicity in fish models. Curr. Pharm. Des. 25:3927–3942
Charlesworth A, Wilczynska A, Thampi P, et al (2006) Musashi regulates the temporal order of mRNA translation during Xenopus oocyte maturation. EMBO J 25:2792–2801. https://doi.org/10.1038/sj.emboj.7601159
Chiu DTY, Stults FH, Tappel AL (1976) Purification and properties of rat lung soluble glutathione peroxidase. Biochim Biophys Acta - Enzymol 445:558–566. https://doi.org/10.1016/0005-2744(76)90110-8
Cho YS, Lee SY, Bang IC, et al (2009) Genomic organization and mRNA expression of manganese superoxide dismutase (Mn-SOD) from *Hemibarbus mylodon* (Teleostei, Cypriniformes). Fish Shellfish Immunol 27:571–576. https://doi.org/10.1016/j.fsi.2009.07.003
Choi JS, Kim RO, Yoon S, Kim WK (2016) Developmental toxicity of zinc oxide nanoparticles to zebrafish (*Danio rerio*): A transcriptomic analysis. PLoS One 11:e0160763. https://doi.org/10.1371/journal.pone.0160763
Choudhury MG, Kumari S, Das KB, Saha N (2018) Lipopolysaccharide causes NFκB-mediated induction of inducible nitric oxide synthase gene and more production of nitric oxide in air-breathing catfish, *Clarias magur* (Hamilton). Gene 658:18–27. https://doi.org/10.1016/j.gene.2018.03.018
Choudhury MG, Saha N (2012) Influence of environmental ammonia on the production of nitric oxide and expression of inducible nitric oxide synthase in the freshwater air-breathing catfish (*Heteropneustes fossilis*). Aquat Toxicol 116–117:43–53. https://doi.org/10.1016/j.aquatox.2012.03.006
Cong Y, Jin F, Wang J, Mu J (2017) The embryotoxicity of ZnO nanoparticles to marine medaka, *Oryzias melastigma*. Aquat Toxicol 185:11–18. https://doi.org/10.1016/j.aquatox.2017.01.006
de Castro E, Sigrist CJA, Gattiker A, et al (2006) ScanProsite: detection of PROSITE signature matches and ProRule-associated functional and structural residues in proteins. Nucleic Acids Res 34:W362–W365. https://doi.org/10.1093/nar/gkl124
DeLeve LD, Kaplowitz N (1991) Glutathione metabolism and its role in hepatotoxicity. Pharmacol Ther 52:287–305. https://doi.org/https://doi.org/10.1016/0163-7258(91)90029-L
Dorval J (2003) Role of glutathione redox cycle and catalase in defense against oxidative stress induced by endosulfan in adrenocortical cells of rainbow trout (*Oncorhynchus mykiss*). Toxicol Appl Pharmacol 192:191–200. https://doi.org/10.1016/S0041-008X(03)00281-3
Ellman GL (1959) Tissue sulfhydryl groups. Arch Biochem Biophys 82:70–77. https://doi.org/10.1016/0003-9861(59)90090-6
Fu PP, Xia Q, Hwang HM, et al (2014) Mechanisms of nanotoxicity: Generation of reactive oxygen species. J Food Drug Anal 22:64–75. https://doi.org/10.1016/j.jfda.2014.01.005
Fukasawa Y, Tsuji J, Fu SC, et al (2015) MitoFates: improved prediction of mitochondrial targeting sequences and their cleavage sites. Mol Cell proteomics 14:1113–1126. https://doi.org/10.1074/mcp.M114.043083
Gasteiger E, Hoogland C, Gattiker A, et al (2005) Protein Identification and Analysis Tools on the ExPASy Server. In: Walker J (ed) The Proteomics Protocols Handbook SE - 52. Humana Press, Totowa, NJ, pp 571–607
Guan R, Kang T, Lu F, et al (2012) Cytotoxicity, oxidative stress, and genotoxicity in human hepatocyte and embryonic kidney cells exposed to ZnO nanoparticles. Nanoscale Res Lett 7:602. https://doi.org/10.1186/1556-276X-7-602
Habig WH, Pabst MJ, Jakoby WB (1974) Glutathione S-transferases. The first enzymatic step in mercapturic acid formation. J Biol Chem 249:7130–9
Halliwell B (1999) Antioxidant defence mechanisms: From the beginning to the end (of the beginning). Free Radic Res 31:261–272. https://doi.org/10.1080/10715769900300841
Halvorsen M, Martin JS, Broadaway S, Laederach A (2010) Disease-associated mutations that alter the RNA structural ensemble. PLoS Genet 6:e1001074. https://doi.org/10.1371/journal.pgen.1001074
Handy RD, Al-Bairuty G, Al-Jubory A, et al (2011) Effects of manufactured nanomaterials on fishes: a target organ and body systems physiology approach. J Fish Biol 79:821–853. https://doi.org/10.1111/j.1095-8649.2011.03080.x
Handy RD, Owen R, Valsami-Jones E (2008) The ecotoxicology of nanoparticles and nanomaterials: Current status, knowledge gaps, challenges, and future needs. Ecotoxicology 17:315–325. https://doi.org/10.1007/s10646-008-0206-0
Hanna SK, Miller RJ, Muller EB, et al (2013) Impact of engineered zinc oxide nanoparticles on the individual performance of *Mytilus galloprovincialis*. PLoS One 8:e61800. https://doi.org/10.1371/journal.pone.0061800
Hansen MN, Jensen FB (2010) Nitric oxide metabolites in goldfish under normoxic and hypoxic conditions. J Exp Biol 213:3593–3602. https://doi.org/10.1242/jeb.048140
Hao L, Chen L (2012) Oxidative stress responses in different organs of carp (*Cyprinus carpio*) with exposure to ZnO nanoparticles. Ecotoxicol Environ Saf 80:103–110. https://doi.org/10.1016/j.ecoenv.2012.02.017
Hasan R, Koner D, Khongmawloh E, Saha N (2020) Induction of nitric oxide synthesis: a strategy to defend against high environmental ammonia-induced oxidative stress in primary hepatocytes of air-breathing

catfish, *Clarias magur*. J Exp Biol 223:jeb219626. https://doi.org/10.1242/jeb.219626
Holmgren A, Bjornstedt M (1995) Thioredoxin and thioredoxin reductase. In: Methods in enzymology. United States, pp 199–208
Kahru A, Dubourguier HC (2010) From ecotoxicology to nanoecotoxicology. Toxicology 269:105–119. https://doi.org/https://doi.org/10.1016/j.tox.2009.08.016
Kanzok SM (2001) Substitution of the thioredoxin system for glutathione reductase in *Drosophila melanogaster*. Science 291:643–646. https://doi.org/10.1126/science.291.5504.643
Kao YY, Chiung YM, Chen YC, et al (2012) Zinc oxide nanoparticles interfere with zinc ion homeostasis to cause cytotoxicity. Toxicol Sci 125:462–472. https://doi.org/10.1093/toxsci/kfr319
Kaya H, Aydin F, Gürkan M, et al (2015) Effects of zinc oxide nanoparticles on bioaccumulation and oxidative stress in different organs of tilapia (*Oreochromis niloticus*). Environ Toxicol Pharmacol 40:936–947. https://doi.org/10.1016/j.etap.2015.10.001
Kaya H, Aydın F, Gürkan M, et al (2016) A comparative toxicity study between small and large size zinc oxide nanoparticles in tilapia *(Oreochromis niloticus)*: Organ pathologies, osmoregulatory responses and immunological parameters. Chemosphere 144:571–582. https://doi.org/10.1016/j.chemosphere.2015.09.024
Knowles RG, Salter M (1998) Measurement of NOS activity by conversion of radiolabeled arginine to citrulline using ion-exchange separation. In: Nitric Oxide Protocols, Titheradge M (ed) Humana Press, New Jersey, pp 67–74
Kohen R, Nyska A (2002) Oxidation of biological systems: oxidative stress phenomena, antioxidants, redox reactions, and methods for their quantification. Toxicol Pathol 30:620–650. https://doi.org/10.1080/0192623029016672
Koner D, Banerjee B, Hasan R, Saha N (2019) Antioxidant activity of endogenously produced nitric oxide against the zinc oxide nanoparticle-induced oxidative stress in primary hepatocytes of air-breathing catfish, *Clarias magur*. Nitric Oxide - Biol Chem 84:7–15. https://doi.org/10.1016/j.niox.2018.12.010
Kumari S, Choudhury MG, Saha N (2019) Hyper-ammonia stress causes induction of inducible nitric oxide synthase gene and more production of nitric oxide in air-breathing magur catfish, *Clarias magur* (Hamilton). Fish Physiol Biochem 45:907–920. https://doi.org/10.1007/s10695-018-0593-y
Laskowski RA, MacArthur MW, Moss DS, Thornton JM (1993) PROCHECK: a program to check the stereochemical quality of protein structures. J Appl Crystallogr 26:283–291
Le SY, Maizel J V. (1997) A common RNA structural motif involved in the internal initiation of translation of cellular mRNAs. Nucleic Acids Res 25:362–369. https://doi.org/10.1093/nar/25.2.362
Lefort V, Longueville JE, Gascuel O (2017) SMS: Smart Model Selection in PhyML. Mol Biol Evol 34:2422–2424. https://doi.org/10.1093/molbev/msx149
Lemoine F, Correia D, Lefort V, et al (2019) NGPhylogeny.fr: New generation phylogenetic services for non-specialists. Nucleic Acids Res 47:W260–W265. https://doi.org/10.1093/nar/gkz303
Lin CT, Tseng WC, Hsiao NW, et al (2009) Characterization, molecular modelling and developmental expression of zebrafish manganese superoxide dismutase. Fish Shellfish Immunol 27:318–324. https://doi.org/10.1016/j.fsi.2009.05.015
Lin D, Tian X, Wu F, Xing B (2010) Fate and transport of engineered nanomaterials in the environment. J Environ Qual 39:1896–1908. https://doi.org/10.2134/jeq2009.0423
Liu H, He J, Chi C, Gu Y (2015) Identification and analysis of icCu/Zn-SOD, Mn-SOD and ecCu/Zn-SOD in superoxide dismutase multigene family of *Pseudosciaena crocea*. Fish Shellfish Immunol 43:491–501. https://doi.org/10.1016/j.fsi.2015.01.032
Liu Z, Liu S, Yao J, et al (2016) The channel catfish genome sequence provides insights into the evolution of scale formation in teleosts. Nat Commun 7:11757. https://doi.org/10.1038/ncomms11757
Livak KJ, Schmittgen TD (2001) Analysis of relative gene expression data using real-time quantitative PCR and the $2^{-\Delta\Delta CT}$ Method. Methods 25:402–408. https://doi.org/10.1006/meth.2001.1262
Lushchak VI (2011) Environmentally induced oxidative stress in aquatic animals. Aquat Toxicol 101:13–30. https://doi.org/10.1016/j.aquatox.2010.10.006
Lushchak VI (2012) Glutathione homeostasis and functions: Potential targets for medical interventions. J Amino Acids 2012:1–26. https://doi.org/10.1155/2012/736837
Lushchak VI, Lushchak LP, Mota AA, Hermes-Lima M (2001) Oxidative stress and antioxidant defenses in goldfish *Carassius auratus* during anoxia and reoxygenation. Am J Physiol - Regul Integr Comp Physiol 280:100–107. https://doi.org/10.1152/ajpregu.2001.280.1.r100
Marchler-Bauer A, Lu S, Anderson JB, et al (2011) CDD: a Conserved Domain Database for the functional annotation of proteins. Nucleic Acids Res 39:D225–D229. https://doi.org/10.1093/nar/gkq1189
Moore RB, Kauffman NJ (1970) Simultaneous determination of citrulline and urea using diacetylmonoxime. Anal Biochem 33:263–272. https://doi.org/10.1016/0003-2697(70)90296-4
Moretti S, Armougom F, Wallace IM, et al (2007) The M-Coffee web server: a meta-method for computing multiple sequence alignments by combining alternative alignment methods. Nucleic Acids Res 35:W645–W648. https://doi.org/10.1093/nar/gkm333

Paoletti F, Aldinucci D, Mocali A, Caparrini A (1986) A sensitive spectrophotometric method for the determination of superoxide dismutase activity in tissue extracts. Anal Biochem 154:536–541. https://doi.org/10.1016/0003-2697(86)90026-6
Pesole G, Liuni S, Grillo G, et al (2000) UTRdb and UTRsite: specialized databases of sequences and functional elements of 5′ and 3′ untranslated regions of eukaryotic mRNAs. Nucleic Acids Res 28:193–196. https://doi.org/10.1093/nar/28.1.193
Prieto AI, Jos A, Pichardo S, et al (2009) Time-dependent protective efficacy of Trolox (vitamin E analog) against microcystin-induced toxicity in tilapia (*Oreochromis niloticus*). Environ Toxicol 24:563–579. https://doi.org/10.1002/tox.20458
Ray PC, Yu H, Fu PP (2009) Toxicity and environmental risks of nanomaterials: Challenges and future needs. J Environ Sci Heal Part C 27:1–35. https://doi.org/10.1080/10590500802708267
Rio DC, Ares M, Hannon GJ, Nilsen TW (2010) Purification of RNA Using TRIzol (TRI Reagent). Cold Spring Harb Protoc 2010:pdb.prot5439. https://doi.org/10.1101/pdb.prot5439
Saha N, Ratha BK (1998) Ureogenesis in Indian air-breathing teleosts: Adaptation to environmental constraints. Comp Biochem Physiol Part A Mol Integr Physiol 120 (2): 195–208. https://doi.org/10.1016/S1095-6433(98)00026-9.
Saha N, Ratha BK (2007) Functional ureogenesis and adaptation to ammonia metabolism in Indian freshwater air-breathing catfishes. Fish Physiol Biochem 33:283–295. https://doi.org/10.1007/s10695-007-9172-3
Sakurai A, Nishimoto M, Himeno S, et al (2005) Transcriptional regulation of thioredoxin reductase 1 expression by cadmium in vascular endothelial cells: Role of NF-E2-related factor-2. J Cell Physiol 203:529–537. https://doi.org/10.1002/jcp.20246
Sarkar S, Mukherjee S, Chattopadhyay A, Bhattacharya S (2017) Differential modulation of cellular antioxidant status in zebrafish liver and kidney exposed to low dose arsenic trioxide. Ecotoxicol Environ Saf 135:173–182. https://doi.org/10.1016/j.ecoenv.2016.09.025
Schwede T, Kopp J, Guex N, Peitsch MC (2003) SWISS-MODEL: an automated protein homology-modeling server. Nucleic Acids Res 31:3381–3385. https://doi.org/10.1093/nar/gkg520
Scown TM, Van Aerle R, Tyler CR (2010) Review: Do engineered nanoparticles pose a significant threat to the aquatic environment. Crit Rev Toxicol 40:653–670. https://doi.org/10.3109/10408444.2010.494174
Sessa WC, Pritchard K, Seyedi N, et al (1994) Chronic exercise in dogs increases coronary vascular nitric oxide production and endothelial cell nitric oxide synthase gene expression. Circ Res 74:349–353
Shahzad K, Khan MN, Jabeen F, et al (2019) Toxicity of zinc oxide nanoparticles (ZnO-NPs) in tilapia (*Oreochromis mossambicus*): tissue accumulation, oxidative stress, histopathology and genotoxicity. Int J Environ Sci Technol 16:1973–1984. https://doi.org/10.1007/s13762-018-1807-7
Shaw BJ, Handy RD (2011) Physiological effects of nanoparticles on fish: A comparison of nanometals versus metal ions. Environ Int 37:1083–1097. https://doi.org/10.1016/j.envint.2011.03.009
Shin YJ, Lee WM, Kwak J Il, An YJ (2018) Dissolution of zinc oxide nanoparticles in exposure media of algae, daphnia, and fish embryos for nanotoxicological testing. Chem Ecol 34:229–240. https://doi.org/10.1080/02757540.2017.1405943
Sigrist CJA, Cerutti L, de Castro E, et al (2010) PROSITE, a protein domain database for functional characterization and annotation. Nucleic Acids Res 38:D161–D166
Sinha AK, Zinta G, AbdElgawad H, et al (2015) High environmental ammonia elicits differential oxidative stress and antioxidant responses in five different organs of a model estuarine teleost (*Dicentrarchus labrax*). Comp Biochem Physiol Part C Toxicol Pharmacol 174–175:21–31. https://doi.org/10.1016/j.cbpc.2015.06.002
Smita S, Gupta SK, Bartonova A, et al (2012) Nanoparticles in the environment: Assessment using the causal diagram approach. Environ Heal A Glob Access Sci Source 11:S13. https://doi.org/10.1186/1476-069X-11-S1-S13
Talavera G, Castresana J, Kjer K, et al (2007) Improvement of phylogenies after removing divergent and ambiguously aligned blocks from protein sequence alignments. Syst Biol 56:564–577
Tan SX, Greetham D, Raeth S, et al (2010) The thioredoxin-thioredoxin reductase system can function in vivo as an alternative system to reduce oxidized glutathione in *Saccharomyces cerevisiae*. J Biol Chem 285:6118–6126. https://doi.org/10.1074/jbc.M109.062844
Townsend DM, Tew KD, Tapiero H (2003) The importance of glutathione in human disease. Biomed Pharmacother 57:145–155. https://doi.org/https://doi.org/10.1016/S0753-3322(03)00043-X
Umasuthan N, Bathige SDNK, Thulasitha WS, et al (2014) Characterization of rock bream (*Oplegnathus fasciatus*) cytosolic Cu/Zn superoxide dismutase in terms of molecular structure, genomic arrangement, stress-induced mRNA expression and antioxidant function. Comp Biochem Physiol Part - B Biochem Mol Biol 176:18–33. https://doi.org/10.1016/j.cbpb.2014.07.004
Valavanidis A, Vlahogianni T, Dassenakis M, Scoullos M (2006) Molecular biomarkers of oxidative stress in aquatic organisms in relation to toxic environmental pollutants. Ecotoxicol Environ Saf 64:178–189. https://doi.org/10.1016/j.ecoenv.2005.03.013
Wang Y, Osatomi K, Nagatomo Y, et al (2011) Purification, molecular cloning, and some properties of a

manganese-containing superoxide dismutase from Japanese flounder (*Paralichthys olivaceus*). Comp Biochem Physiol Part B Biochem Mol Biol 158:289–296. https://doi.org/https://doi.org/10.1016/j.cbpb.2010.12.007

Wigginton NS, Haus KL, Hochella MF (2007) Aquatic environmental nanoparticles. J Environ Monit 9:1306–1316. https://doi.org/10.1039/b712709j

Wong SWY, Leung PTY, Djurišić AB, Leung KMY (2010) Toxicities of nano zinc oxide to five marine organisms: Influences of aggregate size and ion solubility. Anal Bioanal Chem 396:609–618. https://doi.org/10.1007/s00216-009-3249-z

Xiong D, Fang T, Yu L, et al (2011) Effects of nano-scale TiO_2, ZnO and their bulk counterparts on zebrafish: Acute toxicity, oxidative stress and oxidative damage. Sci Total Environ 409:1444–1452. https://doi.org/10.1016/j.scitotenv.2011.01.015

Yang Y, Song Z, Wu W, et al (2020) ZnO quantum dots induced oxidative stress and apoptosis in HeLa and HEK-293T cell lines. Front Pharmacol 11:1–8. https://doi.org/10.3389/fphar.2020.00131

Ye J, Coulouris G, Zaretskaya I, et al (2012) Primer-BLAST: A tool to design target-specific primers for polymerase chain reaction. BMC Bioinformatics 13:134. https://doi.org/10.1186/1471-2105-13-134

Zelko IN, Mariani TJ, Folz RJ (2002) Superoxide dismutase multigene family: A comparison of the CuZn-SOD (SOD1), Mn-SOD (SOD2) and EC-SOD (SOD3) gene structures, evolution and expression. Free Radic Biol Med 33:337–349. https://doi.org/10.3828/rs.2012.10

Zhang Y, Nayak T, Hong H, Cai W (2013) Biomedical applications of zinc oxide nanomaterials. Curr Mol Med 13:1633–1645. https://doi.org/10.2174/1566524013666131111130058

Zhao Y, Xie P, Zhang X (2009) Oxidative stress response after prolonged exposure of domestic rabbit to a lower dosage of extracted microcystins. Environ Toxicol Pharmacol 27:195–199. https://doi.org/https://doi.org/10.1016/j.etap.2008.10.005

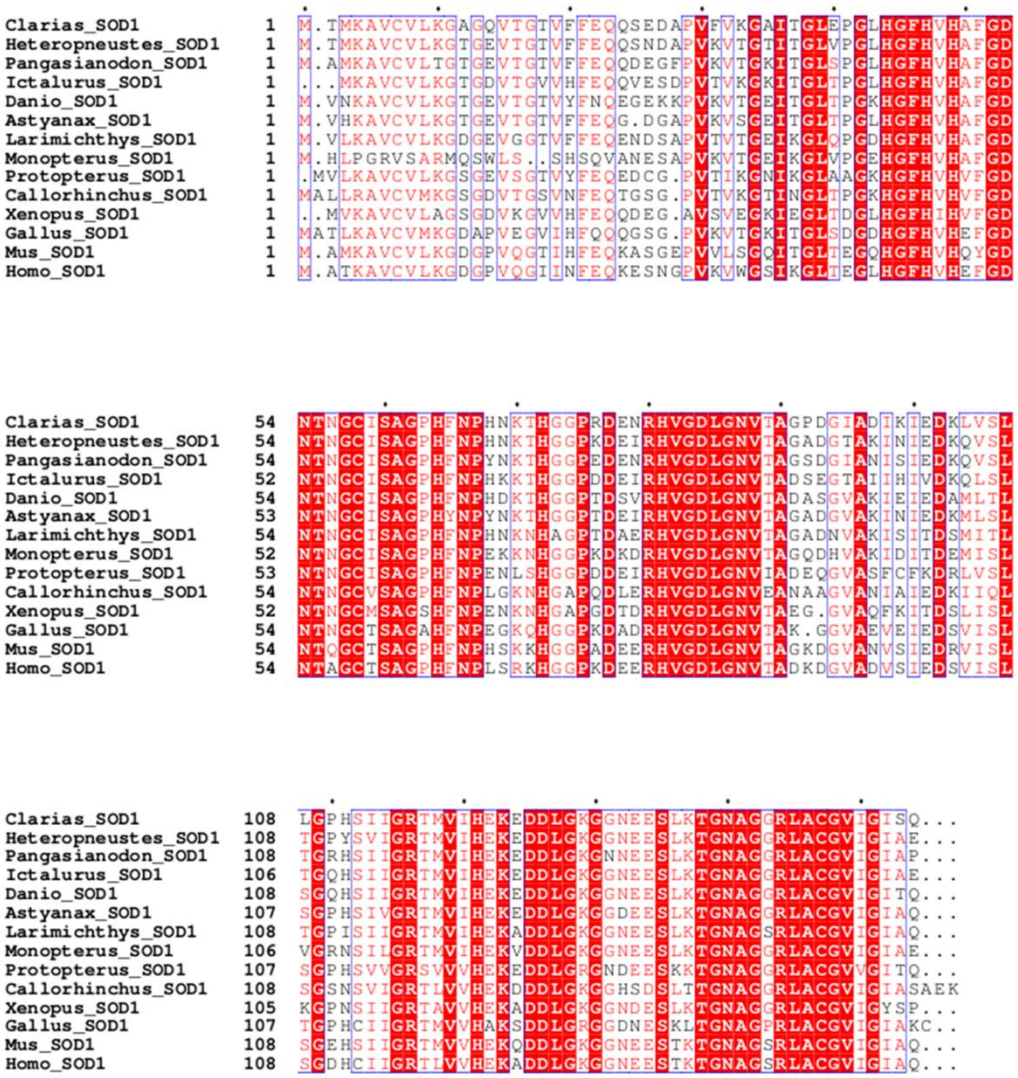

Fig. 1. Multiple alignment of amino acid sequences of SOD1.

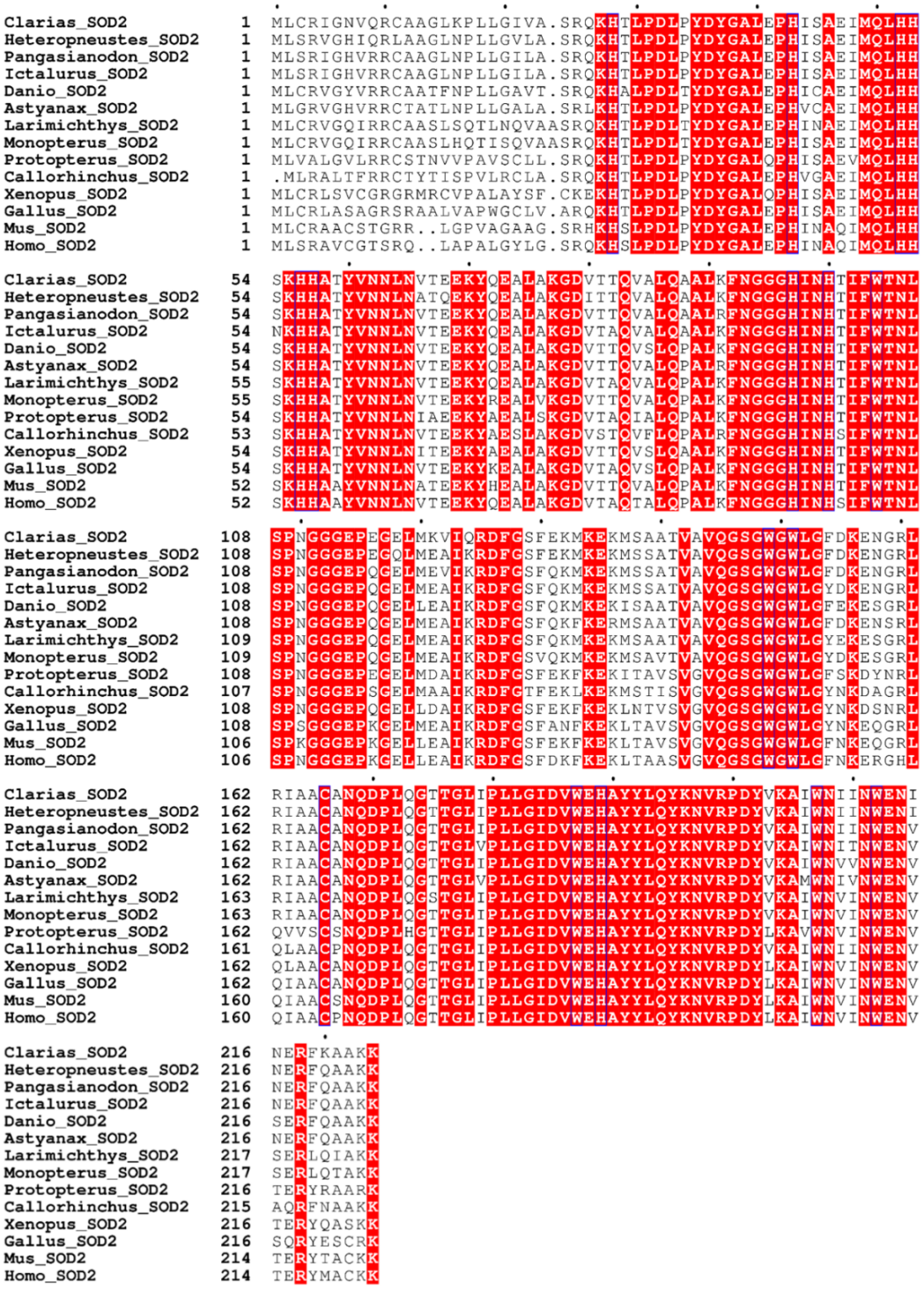

Fig. 2. Multiple alignment of amino acid sequences of SOD2.

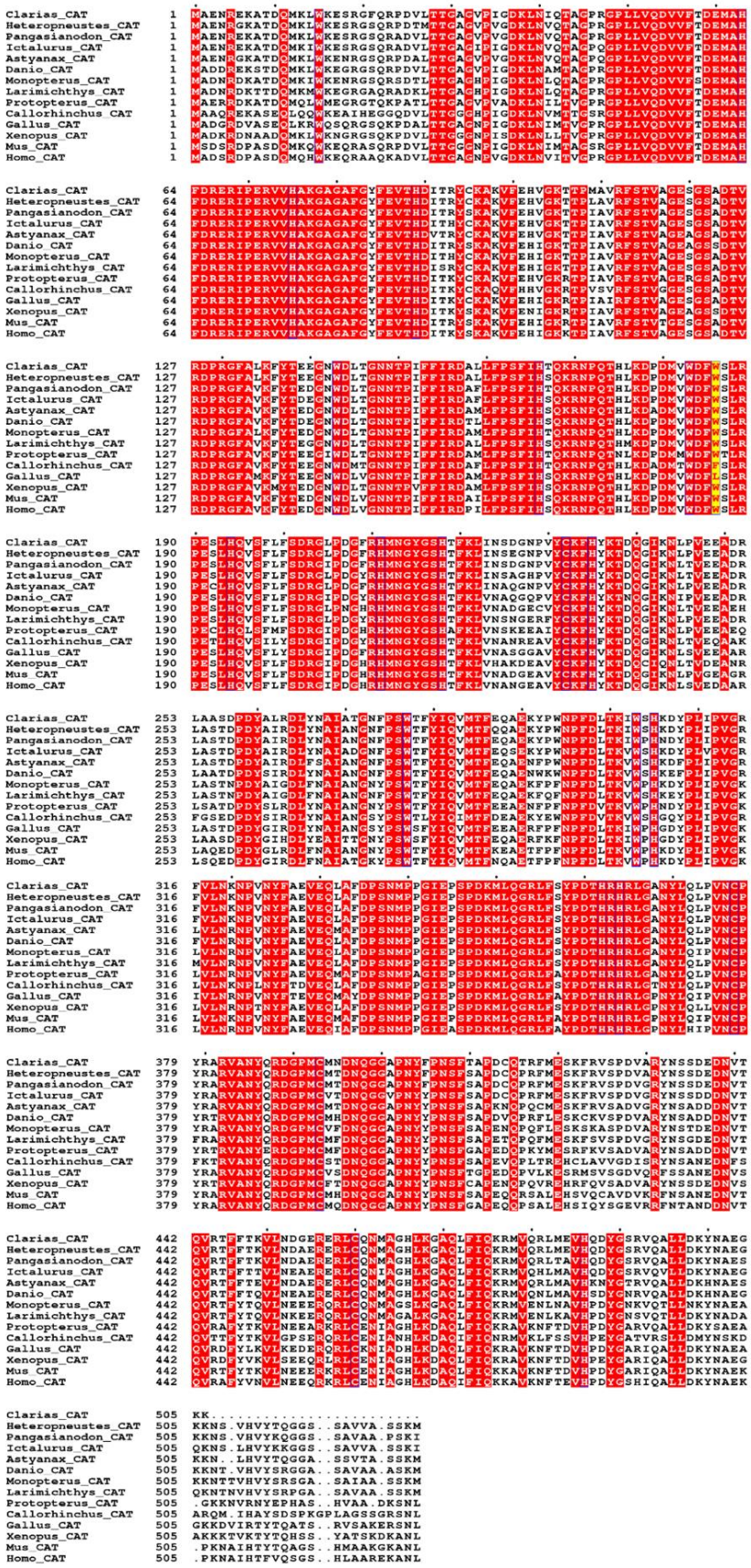

Fig. 3 Multiple alignment of amino acid sequences of CAT.

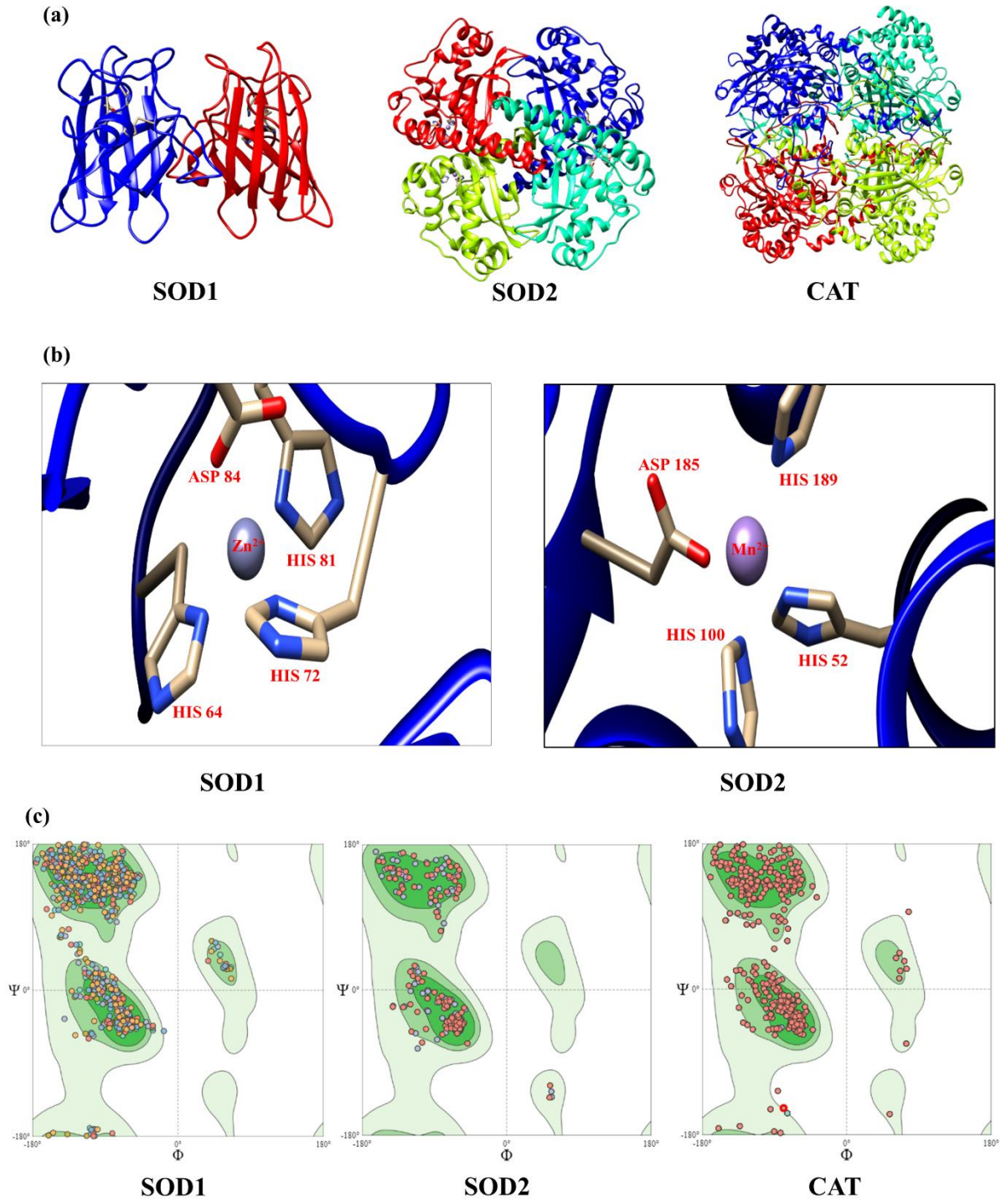

Fig. 4. 3D structure prediction of three antioxidant enzymes, metal binding residues of SOD1 and SOD2, and conformational map (Ramachandran plot) of the psi and phi backbone.

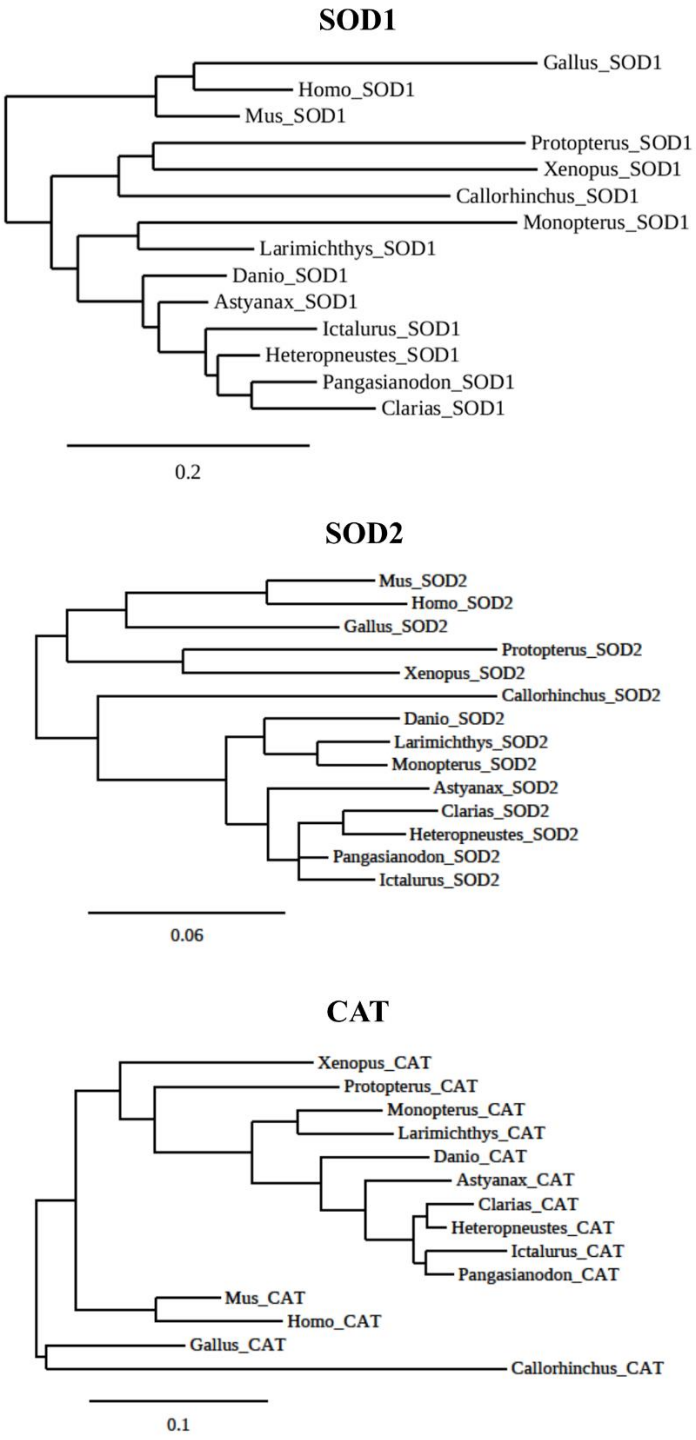

Fig. 5. Phylogenetic tree of amino acid sequences of three antioxidant enzymes.

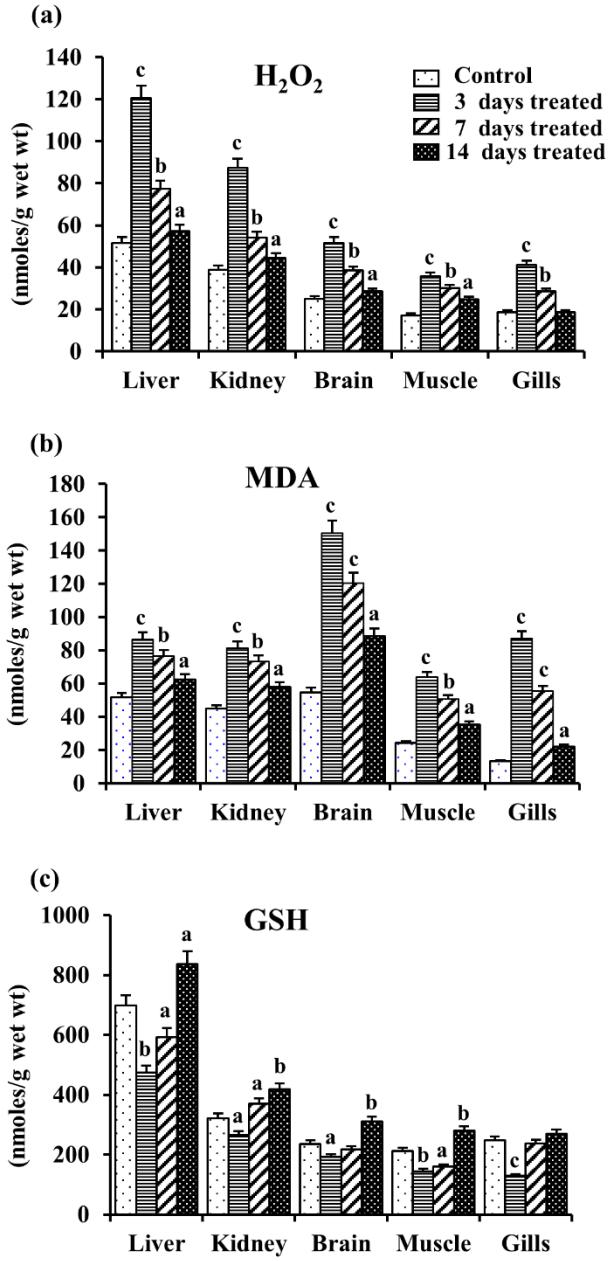

Fig. 6. Effect of ZnO NPs exposure on the concentrations of H_2O_2, MDA and GSH as oxidative biomarkers.

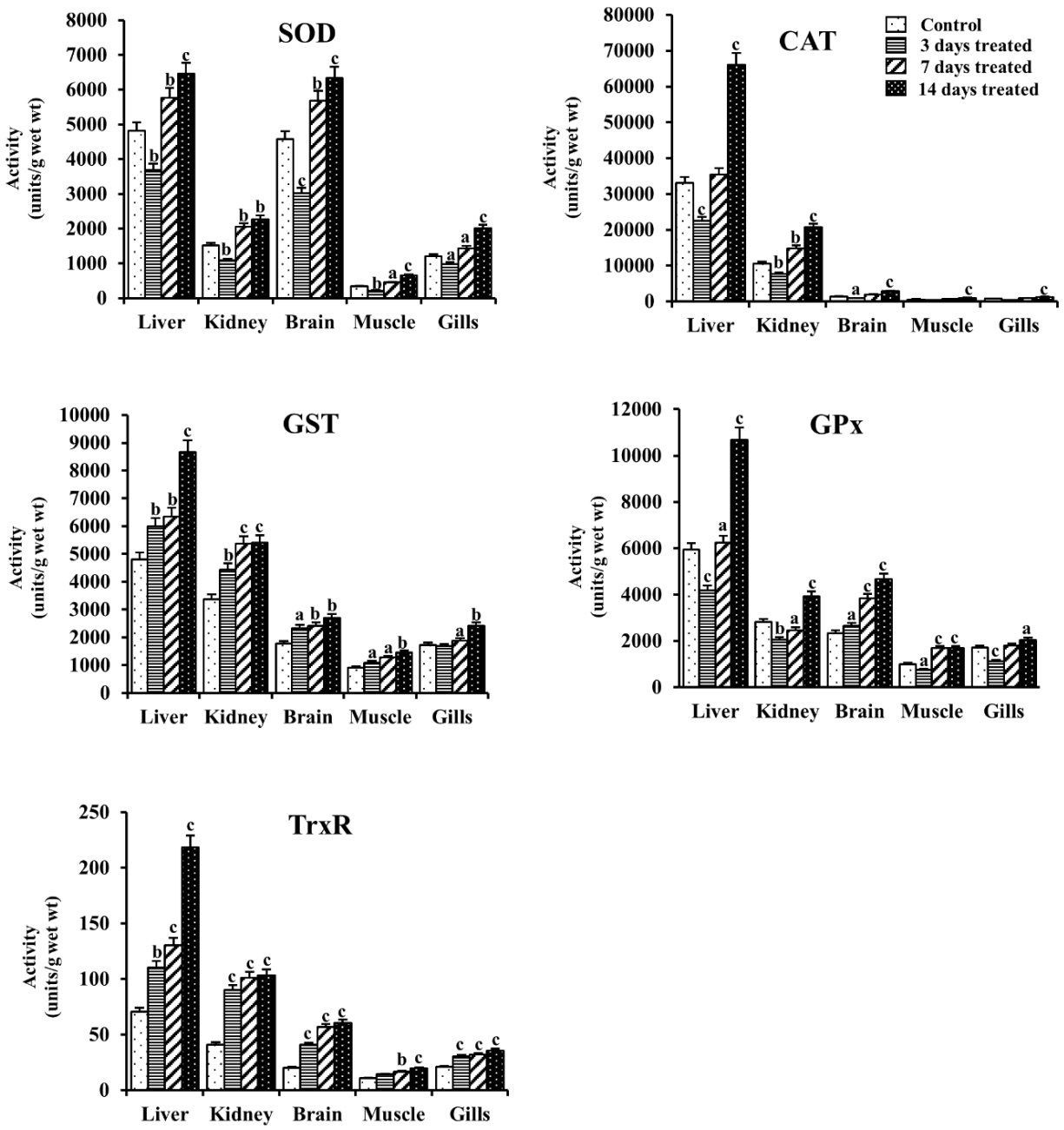

Fig. 7. Effect of ZnO NPs exposure on the activities of antioxidant enzymes.

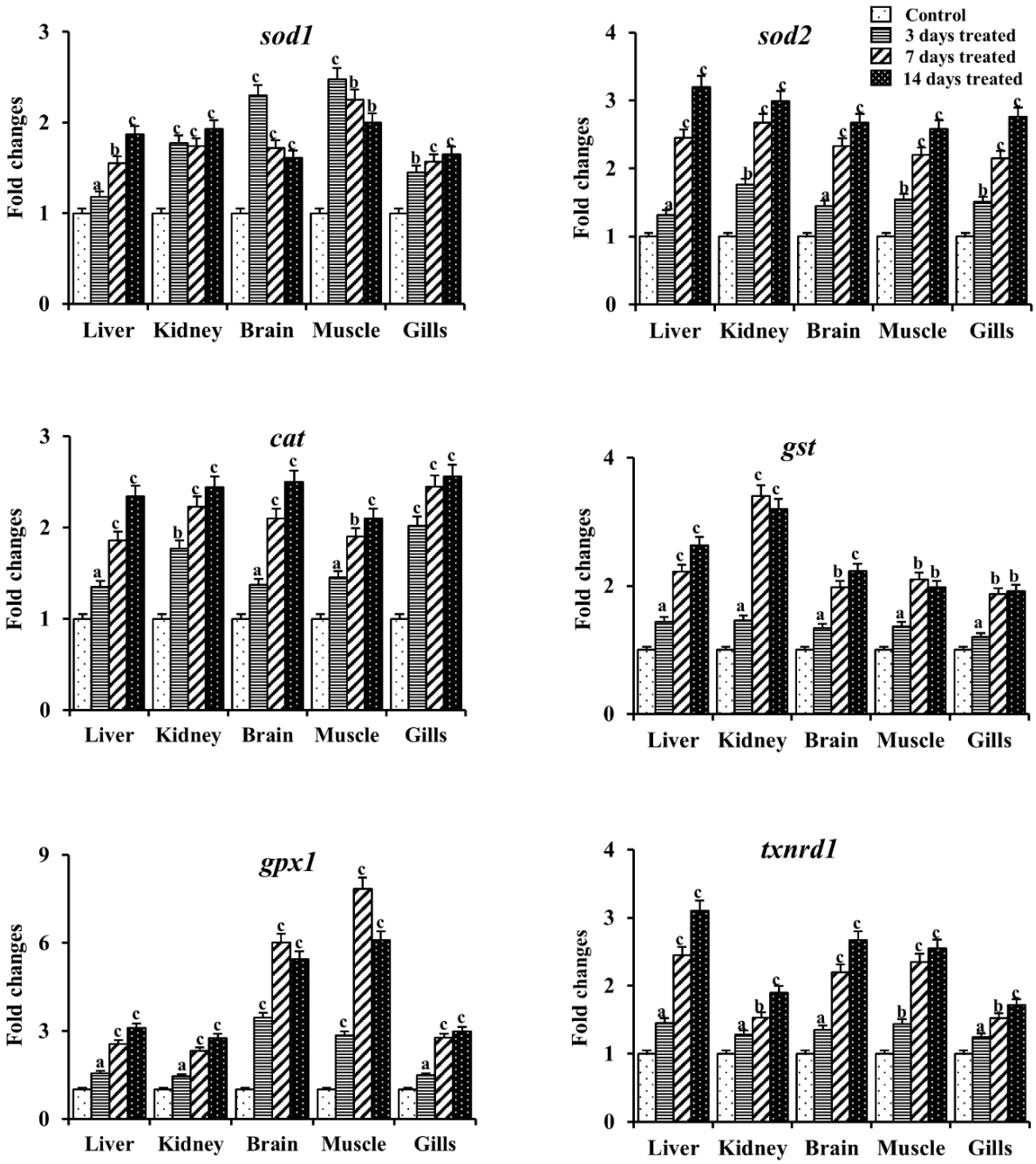

Fig. 8. Effect of ZnO NPs exposure on the expression of mRNAs for different antioxidant enzyme genes.

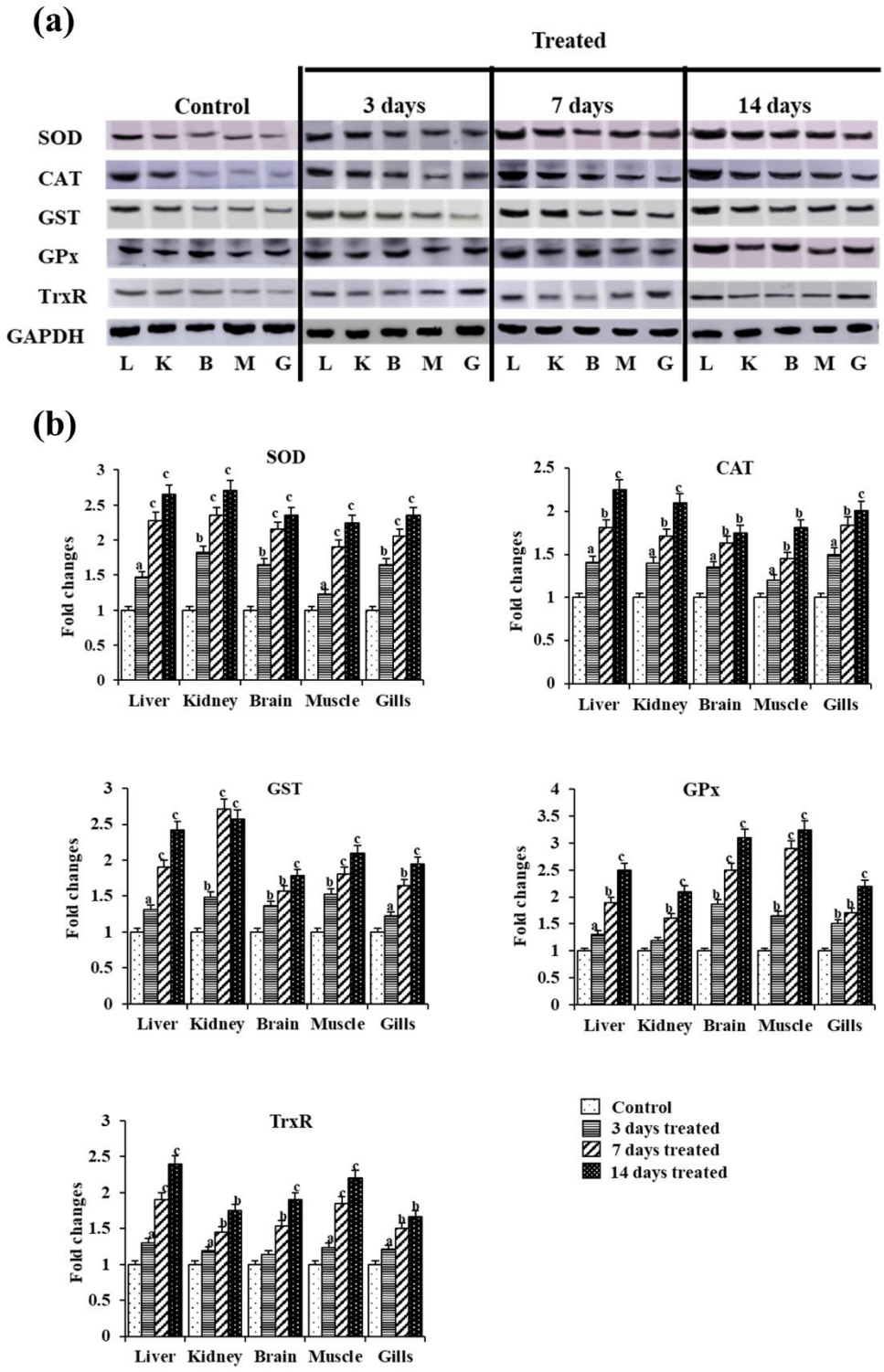

Fig. 9. Effect of ZnO NPs on the expression of different antioxidant enzyme proteins.

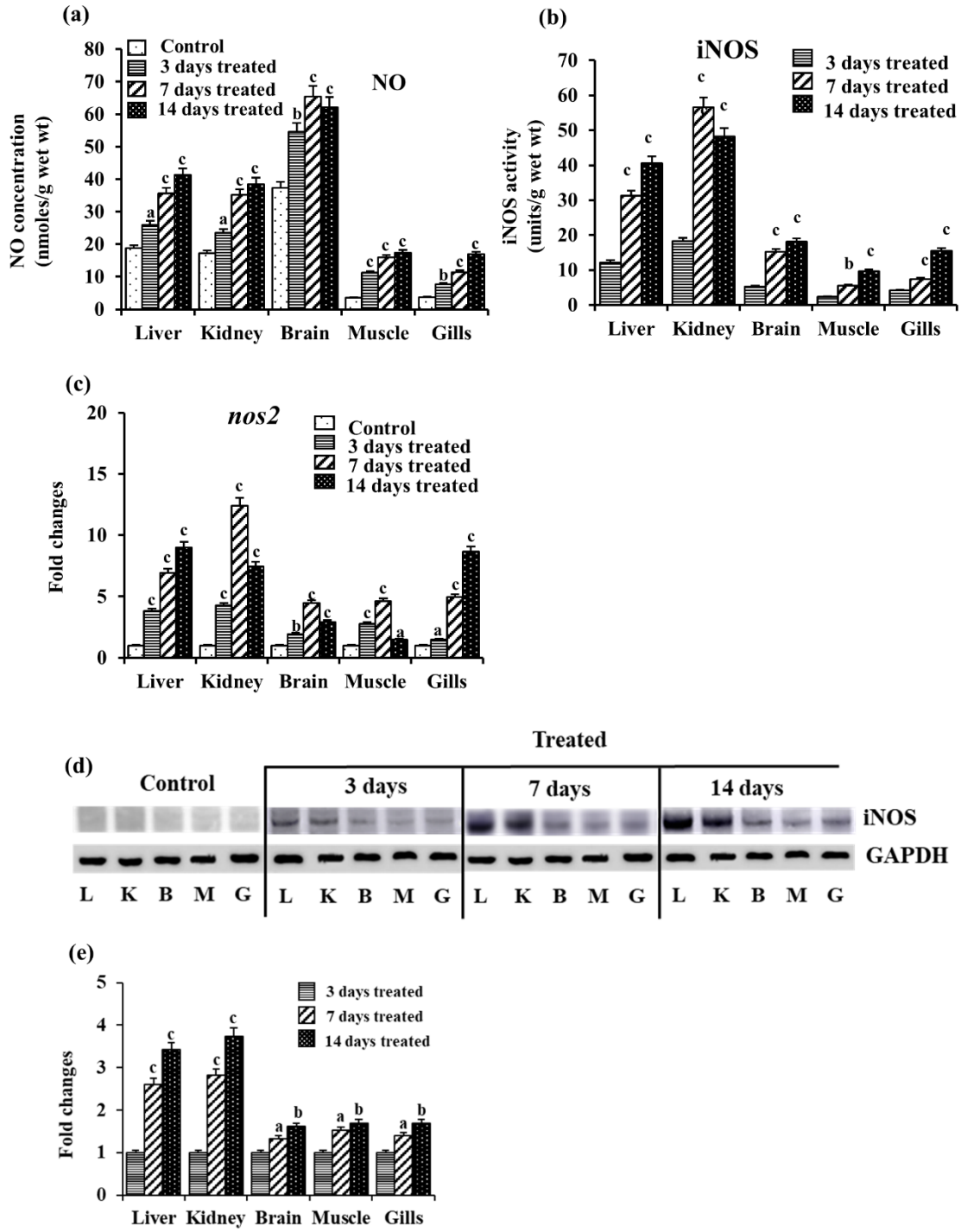

Fig. 10. Effect of ZnO NPs exposure on NO concentration, iNOS activity and its gene expression.

Figure legends

Fig. 1. Multiple alignment of amino acid sequences of SOD1.

Multiple alignments of deduced amino acid sequences of SOD1 from different vertebrates along with *C. magur*. Strictly conserved residues are shaded in red.

Fig. 2. Multiple alignment of amino acid sequences of SOD2.

Multiple alignments of deduced amino acid sequences of SOD2 from different vertebrates along with *C. magur*. Strictly conserved residues are shaded in red.

Fig. 3. Multiple alignment of amino acid sequences of CAT.

Multiple alignments of deduced amino acid sequences of CAT from different vertebrates along with *C. magur*. Strictly conserved residues are shaded in red.

Fig. 4. 3D structure prediction of three antioxidant enzymes, metal binding residues of SOD1 and SOD2, and conformational map (Ramachandran plot) of the psi and phi backbone.

(a) 3D structure prediction of SOD1, SOD2, and CAT found in *C. magur* by SwissModel workspace, (b) the metal binding residues of SOD1, Zn^{2+} (H64, H72, D84 and H81) and SOD2, Mn^{2+} (H52, H100, D185 and H189), (c) conformational map (Ramachandran plot) of the psi and phi backbone. Conformational angles for each residue in the model, where "most favored" (colored in dark green), "generously allowed" (light), and "disallowed" (white) regions are described.

Fig. 5. Phylogenetic tree of amino acid sequences of three antioxidant enzymes.

The phylogenetic trees of SOD1, SOD2, and CAT of *C. magur* were constructed by the maximum likelihood method. Each amino acid sequence at the terminal is presented by the name of the species from which the amino acid sequence originated. The statistical robustness of each tree was estimated by bootstrapping with 1000 replicates. The bar represents the p distance. The accession numbers of all sequences are given in Supplementary table T3.

Fig. 6. Effect of ZnO NPs exposure on the concentrations of H_2O_2, MDA and GSH as oxidative biomarkers.

Changes in the concentrations of (a) hydrogen peroxide (H_2O_2), (b) malondialdehyde (MDA), (c) reduced glutathione (GSH) in different tissues of *C. magur* during exposure to ZnO NPs for 14 days. Values are plotted as mean ± SEM (n=5).

a,b,c: *P* values significant at <0.01,<0.05 and <0.001 levels, respectively, compared to respective controls (one-way ANOVA).

Fig. 7. Effect of ZnO NPs exposure on the activities of antioxidant enzymes.

Changes in the activities of different antioxidant enzymes (SOD, CAT, GST, GPx, and TrxR) in different tissues of *C. magur* during exposure to ZnO NPs for 14 days. Values are plotted as mean ± SEM (n=5).

a,b,c: *P* values significant at <0.01,<0.05 and <0.001 levels, respectively, compared to respective controls (one-way ANOVA).

Fig. 8. Effect of ZnO NPs exposure on the expression of mRNAs for different antioxidant enzyme genes.

qPCR analysis showing changes in the levels of expression of mRNAs for different antioxidant enzyme genes (*sod1*, *sod2*, *cat*, *gst*, *gpx1*, and *txnrd1*) in different tissues of *C. magur* during exposure to ZnO NPs for 14 days. Values are plotted as mean ± SEM (n = 5).

^{a,b,c}: *P* values significant at <0.01,<0.05 and <0.001 levels, respectively, compared to respective controls (one-way ANOVA).

Fig. 9. Effect of ZnO NPs on the expression of different antioxidant enzyme proteins.

(a) Western blot analysis showing changes in the levels of expression of different antioxidant enzyme proteins in different tissues of *C. magur* during exposure to ZnO NPs for 14 days (a representative of 5 individual experiments). (b) Densitometric analysis of different antioxidant enzyme protein concentrations in treated fish compared to untreated controls. Values are plotted as mean ± SEM (n = 5).

a,b,c: *P* values significant at <0.01,<0.05 and <0.001 levels, respectively, compared to respective controls (one-way ANOVA). L – liver, K – kidney, B – brain, M – muscle, G – gills.

Fig. 10. Effect of ZnO NPs exposure on NO concentration, iNOS activity and its gene expression.

(a) Changes in the concentration of NO, (b) changes in the level of iNOS activity, (c) qPCR analysis showing changes in the level of expression of mRNA for *nos2* gene, (d) Western blot analysis showing changes in the level of iNOS protein expression, and (e) densitometric analysis showing fold-changes in the expression of iNOS protein compared to 3 days treated fish in different tissues of *C. magur* during exposure to ZnO NPs for 14 days. Values are plotted as mean ± SEM (n = 5).

a,b,c: *P* values significant at <0.01,<0.05 and <0.001 levels, respectively, compared to respective controls (one-way ANOVA).

L – liver, K – kidney, B – brain, M – muscle, G – gills.

Table 1. Characteristics of full-length cDNAs and encoded ORF of three antioxidant enzyme genes of *C. magur*.

Characteristics	*sod1*	*sod2*	*cat*
Complete CDS (bp)	741	1033	3187
5′ UTR (bp)	76	96	146
ORF bp (amino acids)	465 (154)	675 (224)	1581 (526)
3′ UTR (bp)	201	263	1461
IRES	107, 142	142, 580	446, 672
BRD-Box	-	-	93, 2164
MBE	40, 250, 665	445, 453, 839, 960	40, 74, 498, 516, 1076, 1149
PAS	720-741	1003-1033	-

CDS – coding sequence. UTR – untranslated region. ORF – open reading frame. IRES – internal ribosome entry site. BRD-Box – bearded-box. MBE – Musashi binding element. PAS – polyadenylation signal.

Supplementary Informations

Supplementary Table T1. Primer sets used in the study.

Primers	Forward (5′- 3′)	Reverse (5′- 3′)	Applications
sod1	GCTGTYTGCGTCCTSAAMGG	CCAGAYGACCKCCTGCMTTT	Degenerate PCR
sod2	GACAWGTTCGSAGGTGTRC	ATCTATSCCGMGCAGTGKGA	
cat	GCTGGRGCAGSAGCGTTKG	CAGCSTGCTCARAGGTCATAWC	
sod1-3′-1	CAGGACCTCACTTCAACCCC	AACAGAAGCAGTGACCCTGG	3′- RACE
sod1-3′-2	TGGCTTTCATGTCCATGCCT	GGTCTTGTTGTGGGGGTTGA	
sod1-5′-1	AGTACGCCGTGTTGTCACAT	GGGGTTGAAGTGAGGTCCTG	5′- RACE
sod1-5′-2	CTGTTTGCGTCCTCAAAGGC	AGGCATGGACATGAAAGCCA	
sod2-3′-1	CGGAGCTTCAGTCATAGCCAA	TTTAACCCTGCTGCACACCT	3′- RACE
sod2-3′-2	GCCAACACCAATAACGTGACC	TTAACCCTGCTGCACACCTT	
sod2-5′-1	TCCCACTGCTTGGCATTGAT	TGTGTTGTGTGTGCGCATTT	5′- RACE
sod2-5′-2	TTGCTGCATGTGCAAACCAA	CCACACATCAATGCCAAGCA	
cat-3′-1	TCTGCATCAGGTGTCGTTCC	GTCCAACTGGAATCAGGGGG	3′- RACE
cat-3′-2	CCCTCCGTGACCTGTACAAC	AGCGTCCAACTGGAATCAGG	
cat-5′-1	TTCGGCGTTGCTTGGAATTG	GGGCCATCTCGTCAGTGAAA	5′- RACE
cat-5′-2	GGGGCGGGTCTTAGTAAACG	CAATTCCAAGCAACGCCGAA	

Supplementary Table T2. Primer sets used in the study.

Primers	Forward (5′ -3′)	Reverse (5′ -3′)	Accession No
sod1	AGAGTGAGGATGCTCCCGTA	GCACTGATGCACCCATTTG	(KF444052)
sod2	TCAGCGTGACTTTGGCTCAT	GCCTCCCGTTCTCCTTATCG	(MH891501)
cat	GCTACGGATCCCACACCTTC	GTCACGGAGGGCATAGTCAG	(MW752164)
gst1	GCAAGGGTGAACGAGTACCT	AGCGGCATCCATCTTGTCT	(KC665945)
gpx1	CGCTGAAATACGTCCGTCCT	AGCGTCAATCCCGTTCACAT	(KF414736)
trd1	GGGAGAAGAGAGCACAGCAT	CTTTGAGCACGCAAGACCTC	(KU521854)
nos2	GGATGGACCCCAAAGTACGG	TGGGTGCTCCATTTCAACCT	(KT180212)
β-actin	GCCTCTTCCTCCTCTCTGGA	AGATGGCTGGAAGAGAGCCT	(EU527190)
tuba1	GTCGAGCAAGGTAACGAACTTCAC	GTGGATGGAGATACACTCACGCA	(AB923912)

Supplementary Table T3. INSDC accession numbers for antioxidant enzyme genes from different organisms.

Sequences	Organism (accession number)
SOD1	*Clarias magur* (AGZ94900)
SOD2	*Clarias magur* (AYP27274)
CAT	*Clarias magur* (KAF5908317)
SOD1	*Heteropneustes fossilis* (QCF47161)
SOD2	*Heteropneustes fossilis* (QCF47161)
CAT	*Heteropneustes fossilis* (QCF47162)
SOD1	*Pangasianodon hypophthalmus* (XP_026797864)
SOD2	*Pangasianodon hypophthalmus* (XP_026778834)
CAT	*Pangasianodon hypophthalmus* (XP_026774942)
SOD1	*Ictalurus punctatus* (NP_001187921)
SOD2	*Ictalurus punctatus* (AHH42921)
CAT	*Ictalurus punctatus* (AHH39180)
SOD1	*Danio rerio* (NP_571369)
SOD2	*Danio rerio* (NP_956270)
CAT	*Danio rerio* (NP_570987)
SOD1	*Astyanax mexicanus* (XP_015460818)
SOD2	*Astyanax mexicanus* (XP_015464209)
CAT	*Astyanax mexicanus* (XP_007235106)
SOD1	*Larimichthys crocea* (NP_001290289)
SOD2	*Larimichthys crocea* (NP_001290293)
CAT	*Larimichthys crocea* (XP_010733480.3)
SOD1	*Monopterus albus* (XP_020454068)
SOD2	*Monopterus albus* (XP_020444201)
CAT	*Monopterus albus* (XP_020480641)
SOD1	*Protopterus annectens* (AGV06210)
SOD2	*Protopterus annectens* (AGV06211)
CAT	*Protopterus annectens* (AGV06209)
SOD1	*Callorhinchus milii* (NP_001279423)
SOD2	*Callorhinchus milii* (NP_001279581)
CAT	*Callorhinchus milii* (XP_007903022)
SOD1	*Xenopus laevis* (NP_001359042)
SOD2	*Xenopus laevis* (AAQ63483)
CAT	*Xenopus laevis* (ABK62836)
SOD1	*Gallus gallus* (AAB88059)
SOD2	*Gallus gallus* (NP_989542)
CAT	*Gallus gallus* (NP_001026386)
SOD1	*Mus musculus* (NP_035564)
SOD2	*Mus musculus* (CAJ18481)
CAT	*Mus musculus* (NP_033934)
SOD1	*Homo sapiens* (AAB05662)
SOD2	*Homo sapiens* (NP_001309749)
CAT	*Homo sapiens* (NP_001743)